

## **Reduced Frizzled receptor 4 expression prevents WNT/ $\beta$ -catenin-driven alveolar lung repair in COPD**

Wioletta Skronska-Wasek<sup>1</sup>, Kathrin Mutze<sup>1</sup>, Hoeke A. Baarsma<sup>1</sup>, Ken R. Bracke<sup>2</sup>, Hani N. Alsafadi<sup>1</sup>, Mareike Lehmann<sup>1</sup>, Rita Costa<sup>1</sup>, Mariano Stornaiuolo<sup>3</sup>, Ettore Novellino<sup>3</sup>, Guy G. Brusselle<sup>2</sup>, Darcy E. Wagner<sup>1</sup>, Ali Ö. Yildirim<sup>1</sup>, Melanie Königshoff<sup>1,4</sup>

<sup>1</sup>Comprehensive Pneumology Center, Ludwig Maximilian University, University Hospital Grosshadern, and Helmholtz Zentrum München, Munich, Germany; Member of the German Center of Lung Research (DZL); <sup>2</sup>Department of Respiratory Medicine, Ghent University Hospital, Ghent, Belgium; <sup>3</sup>Department of Pharmacy, University of Naples Federico II, Naples, Italy, <sup>4</sup>Division of Pulmonary Sciences and Critical Care Medicine, Department of Medicine, University of Colorado, Denver.

Corresponding author: melanie.koenigshoff@ucdenver.edu

Division of Pulmonary Sciences and Critical Care Medicine

Department of Medicine, University of Colorado, Denver

AMC, Research 2, 9th Flr, 12700 East 19th Ave, Aurora, CO 80045

### **Author contributions**

W.S.-W., K.M., D.E.W., H.N.A., M.L., R.C. and H.A.B. designed and performed experiments and data analysis; A.Ö.Y. performed animal work; K.R.B. and G.G.B. collected, processed and analyzed human tissue; M.S. and E.N. generated the FzM1 allosteric inhibitor; M.K. oversaw all experimental design and data analysis; W.S.-W., K.M. and M.K. drafted the manuscript;

A.Ö.Y., K.R.B., G.G.B., M.S., E.N., H.A.B. and D.E.W. critically revised the manuscript. All the authors have read, reviewed and approved the final manuscript as submitted to take public responsibility for it.

### **Funding**

This work was funded by a European Research Council Starting Grant to M.K. (ERC-2010-StG 261302) and W2/W3 Professorship Award to M.K. from the Helmholtz Association, Germany. D.E.W. is supported by a Whitaker International Scholar Fellowship and the Helmholtz Munich Postdoctoral Program. H.A.B. is supported by the European Respiratory Society Fellowship and the Helmholtz Munich Postdoctoral Program. M.S. is supported by MFAG (2015 Id. 17651).

**Competing financial interests:** The authors declare no competing financial interests.

**Key words:** emphysema, regeneration, smoking, cigarette smoke, FZD4

## Abstract

**Rationale:** Chronic obstructive pulmonary disease (COPD), in particular emphysema, is characterized by loss of parenchymal alveolar tissue and impaired tissue repair. WNT/ $\beta$ -catenin signaling is reduced in COPD, however, the mechanisms thereof, specifically the role of WNT receptors Frizzled (FZD), remain unexplored. **Objective:** To identify and functionally characterize specific FZD receptors that control downstream WNT signaling in impaired lung repair in COPD. **Methods:** FZD expression was analyzed in lung homogenates and alveolar epithelial type II (ATII) cells of never-smokers, smokers, and COPD patients, and two experimental COPD models by qRT-PCR, immunoblotting, and immunofluorescence. The functional effects of cigarette smoke on FZD4, WNT/ $\beta$ -catenin signaling, and elastogenic components were investigated in primary ATII cells *in vitro* and 3D lung tissue cultures (3D-LTCs) *ex vivo*. Gain- and loss-of-function approaches were applied to determine the effects of FZD4 signaling on alveolar epithelial cell wound healing and repair, and on expression of elastogenic components. **Measurements and Main Results:** FZD4 expression was reduced in human and experimental COPD lung tissues as well as primary human ATII cells from COPD patients. Cigarette smoke exposure downregulated FZD4 expression *in vitro* and *in vivo*, along with reduced WNT/ $\beta$ -catenin activity. Inhibition of FZD4 decreased WNT/ $\beta$ -catenin-driven epithelial cell proliferation, wound closure and interfered with ATII-to-ATI cell trans-differentiation and organoid formation, which was augmented by FZD4 overexpression. Moreover, FZD4 restoration by overexpression or pharmacological induction led to induction of WNT/ $\beta$ -catenin signaling and expression of elastogenic components in 3D-LTCs *ex vivo*. **Conclusions:** Reduced FZD4 expression in COPD contributes to impaired alveolar repair capacity.

## Introduction

Chronic obstructive pulmonary disease (COPD) is one of the leading causes of death worldwide and is associated with a poor outcome and high socioeconomic burden (1). COPD is characterized by chronic airway inflammation and remodeling as well as loss of parenchymal alveolar tissue, called emphysema (2, 3). COPD initiation and development has been linked to a variety of genetic and environmental insults with cigarette smoking being one of the major risk factors (4). The mechanisms driving disease pathogenesis include oxidative stress, a protease/antiprotease imbalance and altered innate immune response leading to pulmonary inflammation, cell death and alveolar destruction (5-7). More recent data suggest that impaired endogenous lung tissue maintenance and, in particular, damaged alveolar epithelial cell repair processes further contribute to emphysema development and progression, however, the molecular mechanisms are not fully understood (6-9). The identification of novel therapeutic targets that are suitable to induce lung repair is of major interest, as to date no causal therapy is available for this devastating disease. Signal pathways that govern normal lung development represent potential targets. WNT/ $\beta$ -catenin signaling is known to be critical for lung morphogenesis (10, 11). The WNT pathway consists of at least 19 different WNT ligands, which are secreted glycoproteins that can bind to 10 distinct Frizzled (FZD) receptors and low density lipoprotein-related protein (LRP) 5/6 co-receptors (10, 12). WNT signaling can be divided into canonical (i.e.  $\beta$ -catenin dependent) and non-canonical signaling. In the case of canonical WNT/ $\beta$ -catenin signaling, ligand-receptor binding prevents  $\beta$ -catenin phosphorylation, and thus degradation.  $\beta$ -catenin accumulates in the cytoplasm and translocates to the nucleus, where it binds to T-cell specific transcription factor/lymphoid enhancer-binding factor (TCF/LEF). This in turn leads to the expression of various target genes involved, among others, in cell proliferation (12).

We and others have demonstrated that canonical WNT/ $\beta$ -catenin signaling is reduced in the lung epithelium of emphysematous lung tissue from COPD patients (13-16). Activation of WNT/ $\beta$ -catenin by a GSK-3 $\beta$  inhibitor (Lithium Chloride) led to reversal of experimental emphysema *in vivo* (13), and importantly, to alveolar epithelial cell activation in COPD patient-derived 3D lung tissue cultures (3D-LTCs) (14). The mechanism underlying WNT/ $\beta$ -catenin signal reduction in COPD, however, has not yet been explored. Here, we investigated the role of FZD receptors that control downstream WNT signaling. We demonstrate that FZD4 is downregulated by cigarette smoke (CS) in experimental and human COPD, preventing WNT/ $\beta$ -catenin signal activity and thus alveolar tissue repair in COPD. These data suggest that the induction of canonical WNT signaling by targeting the WNT receptor FZD4 in the lung might lead to improved alveolar epithelial cell function and thus represents a potential beneficial approach for tissue repair in COPD patients.

## **Material and Methods**

### **Human lung tissue study population**

Lung resection specimens were obtained from 92 subjects, of which 78 were from surgery for solitary pulmonary tumors (Ghent University Hospital, Ghent, Belgium) and 14 were from explant lungs of end-stage COPD patients undergoing lung transplantation (University Hospital Gasthuisberg, Leuven, Belgium). Lung tissue from the resection specimen was harvested by a pathologist at maximum distance from the tumor. The cohort of 92 patients was divided into 4 subgroups: 18 never smokers, 26 smokers without airflow limitation, 34 patients with COPD GOLD stage II and 14 patients with COPD GOLD stage III-IV (Table 1). Patients were considered ex-smokers when they had ceased smoking for more than 1 year. COPD diagnosis and severity was defined using pre-operative spirometry according to the Global Initiative for Chronic Obstructive Lung Disease (GOLD) classification. All patients with COPD had stable disease as patients with exacerbations within 2 months before the study were excluded. Other exclusion criteria were chemotherapy or radiotherapy in the last 6 months, diagnosis of mesothelioma or asthma and infection of the upper or lower respiratory tract in the preceding 4 weeks. Our study was approved by the medical ethics committee of the Ghent University Hospital (2011/114) and the University Hospital Gasthuisberg (S51577). All subjects provided written informed consent. Primary human alveolar epithelial type II (phATII) cells were isolated from non-COPD (n=7) or COPD (n=3) lung tissue biopsies from the Comprehensive Pneumology Center (CPC) cohort at the University Hospital Grosshadern of the Ludwig Maximilian University (LMU). Participants provided written informed consent to participate in this study, in accordance with approval by the local ethics committee of the LMU, Germany (Project 333-10, 455-12).

## Animals

Six- to eight-week-old pathogen-free female C57BL/6N mice were obtained from Charles River and housed in rooms with constant temperature and humidity with 12h light cycles. Mice had free access to water and rodent chow. For the mouse model of elastase-induced emphysema, pancreatic porcine elastase was dissolved in sterile phosphate-buffered saline and applied orotracheally (80 U/kg body weight) in a total volume of 80  $\mu$ l. Control mice received 80  $\mu$ l of sterile phosphate-buffered saline (PBS). For the mouse model of CS-induced emphysema, animals were exposed to filtered air (FA) or mainstream CS, generated from 3R4F Research Cigarettes (Tobacco Research Institute, University of Kentucky, Lexington, KY, USA), twice per day for 50 minutes, for the indicated time, as described previously (17). Mice were anesthetized and sacrificed at indicated times post-elastase instillation or CS exposure. Lung tissue was flushed, excised, snap-frozen in liquid nitrogen and stored at -80°C until further analyses. All animal studies were conducted under strict governmental and international guidelines and approved by the local government for the administrative region of Upper Bavaria (Project 55.2-1-54-2532-129-14).

## Generation of human and mouse three-dimensional (3D) *ex vivo* lung tissue cultures (LTCs)

Generation of the 3D-LTCs was performed as previously described (14). In brief, for the patient-derived 3D-LTCs, lung segments were cannulated through the bronchus and filled with warm agarose (3 %, A9414; Sigma). Segments were cut with a vibratome (Hyrax V55; Zeiss, Jena, Germany) to 500  $\mu$ m slices (speed 6-10  $\mu$ m/s, frequency of 100 Hz, amplitude 1.2 mm). Slices were treated with FzM1 (2.5  $\mu$ M) or respective DMSO control for 24h or 72h in sterile medium (DMEM/Ham's F12; Gibco, supplemented with 100 U/ml penicillin, 100  $\mu$ g/ml streptomycin and 2.5  $\mu$ g/ml amphotericin B; Sigma). For murine 3D-LTCs, healthy six-

to eight-week-old pathogen-free female C57BL/6N mice were used. Lungs were flushed via the heart with sterile sodium chloride solution and filled with warm, low gelling temperature agarose (2 %) in sterile medium (DMEM/Ham's F12). Further, lobes were cut with a vibratome to a thickness of 300  $\mu$ m slices (speed 10–12  $\mu$ m/s, frequency 80 Hz, amplitude of 1 mm). 3D-LTCs were treated with FzM1 (2.5  $\mu$ M), valproic acid (VA 0.5 mM; Sigma Aldrich P4543), combination of FzM1 and VA or respective DMSO control for 24h or 72h in sterile cultivation medium containing 0.1% FCS. RNA was isolated and gene expression was analyzed by qPCR. Supernatants were collected and stored at -80°C before analysis.

**Detailed description of material and methods, including cigarette smoke extract preparation, cell culture and functional readouts can be found in the Supplemental Methods.**



## Results

### FZD4 is expressed by the alveolar epithelium and decreased in COPD

We first analyzed the expression of all FZD receptors in the mouse model of elastase-induced emphysema, which has been previously shown to exhibit reduced WNT/ $\beta$ -catenin signaling (13) (Fig. 1A). We found that in particular *Fzd4* and *Fzd7* expression was significantly decreased. *Fzd4* and *Fzd7* transcripts were also highly expressed in primary mouse alveolar epithelial type II (pmATII) cells and we detected FZD4 protein in cultured pmATII cells (Supplementary Fig. E1A and E1B). In order to elucidate the potential clinical relevance for altered FZD expression, we further screened for FZD expression in available microarray datasets from whole lung homogenates (GSE47460) as well as primary human alveolar epithelial type II (phATII) cell isolates from COPD and non-COPD patients (18). In both data sets, *FZD4*, but not *FZD7*, were significantly reduced (Supplementary Fig. E1C and E1D, respectively). We detected FZD4 protein expression on healthy phATII cells (Fig. 1B) and confirmed *FZD4* reduction in phATII cells obtained from lung tissue explants from COPD patients compared to donors (Fig. 1C, relative *FZD4* mRNA expression (mean  $\pm$  s.d.): non-COPD  $-1.2 \pm 0.38$ , COPD  $-2.36 \pm 0.35$ ,  $P=0.106$ ). Notably, we confirmed *FZD4* reduction in a large cohort of patients with COPD ( $n=48$ ) compared to never-smokers ( $n=18$ ) as well as for severe COPD ( $n=14$ ) compared to smokers without COPD ( $n=26$ ) (Fig. 1D). *FZD4* mRNA expression further positively correlated with lung function (% FEV1, post-bronchodilator) (Fig. 1E and Supplementary Fig. E2E) and negatively correlated with smoking pack years (Fig. 1F) and aging (Supplementary Fig. E2) in this cohort (even when excluding samples from non-cancerous GOLD IV patients, as presented in Supplementary Fig. E2). In line with this, we observed that oxidative stress-induced senescence reduced *Fzd4* in epithelial cells *in vitro* (Supplementary Fig. E1E).

We thus focused our further studies on FZD4 as a potential receptor contributing to impaired tissue repair observed in COPD pathogenesis.

### **FZD4 expression is downregulated by cigarette smoke (CS) *in vivo* and *in vitro*.**

Given that cigarette smoking is an important risk factor for COPD, and our data suggesting a link between CS and FZD4 expression (Fig. 1D and F), we next addressed if FZD4 is regulated by CS *in vivo* and *in vitro*. We found reduced *Fzd4* receptor mRNA expression in lung homogenates from mice exposed to CS compared to filtered air (FA) at early (3 days) as well as late (4 months) time points (Fig. 2A, relative *Fzd4* mRNA expression (mean  $\pm$  s.d.): FA 3d  $2.13 \pm 0.1$ , CS 3d  $1.35 \pm 0.19$ , FA 4m  $1.49 \pm 0.09$ , CS 4m  $0.5 \pm 0.14$ ). At baseline, *Fzd4* mRNA expression was also significantly reduced over time (Fig. 2A), and in old *versus* young mice (Supplementary Fig. E3A), suggesting a potential aging-associated reduction. In agreement with the mRNA expression, we found reduced FZD4 protein as early as 3 days upon CS exposure as analyzed by immunoblotting, suggesting an immediate effect of CS on FZD4 expression, which was accompanied by reduced active  $\beta$ -catenin (ABC) protein expression (Fig. 2B). Similarly, we found reduced FZD4 expression in the alveolar epithelium in tissue specimens of smokers compared to non smokers (Supplementary Fig. E3B). In order to investigate the effect of CS in more detail, we exposed primary mouse alveolar epithelial type II (pmATII) cells directly to CS extract (CSE) (Fig. 2D, E). CSE led to the induction of the well-known marker *Cyp1a1* as well as reduction of *Sparg* expression (19) in pmATII cells (Fig. 2D). Moreover, WNT/ $\beta$ -catenin target gene *Axin2* and *Fzd4* mRNA expression were decreased upon stimulation with CSE in pmATII cells as well as in MLE12 cells (Fig. 2D and Supplementary Fig. E3C, respectively) (Fig. 2D, fold change (relative mRNA expression (mean  $\pm$  s.d.): *Axin2*  $-1.44 \pm 0.25$ , *Fzd4*  $-1.66 \pm 0.71$ ,  $P < 0.01$ ). FZD4 was also reduced on protein

level in pmATII cells upon CSE exposure, as assessed by immunofluorescence staining (Fig. 2E, FZD4 expression relative to DAPI, % of 0% CSE (100%) (mean + s.d.): 25% CSE 76±10%,  $P<0.05$ ) and immunoblotting (Supplementary Fig. E3D).

### **FZD4 is a positive regulator of canonical WNT signaling**

Given that CS exposure reduced FZD4 expression along with decreased WNT/ $\beta$ -catenin signal activity in alveolar epithelial cells, we next aimed to elucidate if FZD4 expression directly influences WNT/ $\beta$ -catenin signal activity. To this end, we used the recently described inhibitor FzM1, which is an allosteric ligand of FZD4, described to hamper FZD4-Dishevelled complex that is required for  $\beta$ -catenin nuclear translocation (20). Treatment of pmATII cells with FzM1 led to decreased WNT/ $\beta$ -catenin signaling, as analyzed by target gene expression (*Axin2*, *Lgr5*) (Fig. 3A, log fold change (mean + s.d.): *Axin2* -1.76±0.59, *Lgr5* -2.12±0.82,  $P<0.05$ ). In line with these findings, FzM1-mediated inhibition of FZD4 led to the attenuation of WNT3A-induced TCF/LEF-dependent gene transcription in MLE12 cells (Fig. 3B, TOP/FOP activation, fold of control (mean + s.d.): FzM1 1.46±0.8, WNT3A 8.55±2.3, FzM1+WNT3A 2±1.2,  $P<0.01$ ). Furthermore, FzM1 decreased ABC level and reduced LRP6 phosphorylation (pLRP6) upon WNT3A treatment in MLE12 cells, as assessed by immunoblotting (Fig. 3C). Moreover, we also found decreased *AXIN2* expression by FzM1 in 3D human lung tissue cultures (3D-LTCs) *ex vivo* (Supplementary Fig. E4A). We further corroborated our findings using a gain-of-function approach (Fig. 3D and Supplementary Fig. E5). Overexpression of FZD4 led to enhanced WNT/ $\beta$ -catenin signal activity upon WNT3A stimulation in MLE12 cells (Fig. 3D, TOP/FOP activation FZD4 overexpression (OE) compared to empty vector (EV) (mean + s.d.): OE 1.3±0.11, EV+WNT3A

3.5+1.6, OE+WNT3A 12.1+2.5,  $P<0.001$ ). Altogether, these data suggest that FZD4 is a direct regulator of canonical WNT signaling in the mouse and human alveolar epithelium.

### **FZD4 expression regulates alveolar epithelial wound healing and repair**

Canonical WNT signaling has been implicated in lung repair, therefore we next investigated the role of FZD4 on alveolar epithelial cell function. We assessed cellular proliferation and wound healing, crucial processes involved in tissue repair upon gain- and loss-of-function of FZD4. Inhibition of FZD4 signaling by FzM1 led to decreased cell viability (Fig. 4A, compared to 100% control (mean + s.d.): FzM1 73+7%,  $P<0.001$ ), decreased total cell counts (Fig. 4B, compared to 100% control (mean + s.d.): FzM1 62+17.6%,  $P<0.05$ ), reduction of Ki67 in MLE12 cells (Fig. 4D, % of FZD4 positive cells (mean + s.d.): control 78.8+0.01%, FzM1 67.6+3%,  $P<0.05$ ). In addition, FzM1 significantly delayed wound closure in a scratch assay (Fig. 4F, closed scratch in % (mean + s.d.): Control 73.1+2.9%, FzM1 44.3+6.5%,  $P<0.05$ ). These data were further confirmed by FZD4 overexpression which led to increased cell viability (Fig. 4C, FZD4 OE compared to EV (mean + s.d.): 123.6+11.6%,  $P<0.01$ ), percentage of Ki67 positive cells (Fig. 4E, % of FZD4 positive cells (mean + s.d.): EV 45.5+0.9%, OE 56.7+6.4%,  $P<0.05$ ) as well as accelerated wound closure (Fig. 4G, closed scratch in % (mean + s.d.): EV 74.9+10.3%, OE 80.7+10.4%,  $P<0.01$ ).

ATII cells are capable of self-renewal and exert progenitor function for ATI cells upon alveolar epithelial injury. We next elucidated whether FZD4 expression impacts ATII cell marker expression, trans-differentiation and organoid formation. FZD4 inhibition by FzM1 led to a reduction of alveolar epithelial cell marker transcripts, such as *E-cadherin* and the ATI cell marker *T1α* (Supplementary Fig. E6A). Moreover, in the well-characterized *in vitro* model, in which ATII cells spontaneously activate WNT/ $\beta$ -catenin signaling and trans-

differentiate into ATI-like cells during primary culture *in vitro* (21, 22), we observed that blocking of FZD4 by FzM1 led to a significant decrease of the ATI cell marker T1 $\alpha$  on protein level. This was accompanied by decreased ABC and pLRP6 (both indicators of WNT/ $\beta$ -catenin activity) (Fig. 5A), indicating that loss of FZD4 activity results in a defect of ATII-to-ATI cell trans-differentiation, which is presumably mediated by reduced canonical WNT signaling. In addition, we observed a significantly lower number of organoids formed by ATII cells upon FzM1 treatment (Supplementary Fig. E6B). Altogether, these results indicate that FZD4 acts as a positive regulator of lung epithelial wound healing, (trans)differentiation, and organoid formation, and thus might be a potential regulator of tissue repair in the lung.

#### **FZD4 regulates WNT/ $\beta$ -catenin-driven repair and elastogenic components**

WNT/ $\beta$ -catenin signaling has been recently linked to extracellular and elastin remodeling (14, 23). Loss of elastic fibers from small airways and alveolar walls represents a main feature of COPD and elastin, which constitutes the main component of elastic fibers (24), has been shown to be regulated by cigarette smoke (25). Notably, we detected decreased elastin (*Eln*) gene expression induced by CS both, in whole lung homogenate *in vivo* and in epithelial cells *in vitro* (Fig. 6A and 6B, C respectively). While lung epithelial cells most likely do not present the main source of elastin, protein was also detected in cultured ATII cells (Supplementary Fig. E7A), suggesting that they might contribute to the elastic matrix upon injury. We further analyzed expression of elastogenic components and found that both CSE and FZD4 inhibition by FzM1 reduced gene expression of elastin fiber genes, such as *Eln*, Insulin-like growth factor 1 (*Igf1*), Lysyl Oxidase (*Lox*), Lysyl Oxidase Like 1 (*Loxl*), Fibulin1 (*Fbln1*) and Fibulin 5 (*Fbln5*) (26) (Fig. 6C and 6D, respectively) in pmATII cells. Remarkably, IGF1, which has been implicated in elastogenesis processes and shown to be

secreted by ATII cells in previous studies (27, 28) was also significantly reduced on protein level upon CSE as well as FZD4 inhibition in pmATII cells (Fig. 6E and 6F). Furthermore, we confirmed decreased expression of both *Eln* and *Igf1* in *ex vivo* 3D-LTCs upon CSE and FzM1 treatment (Fig. 6G and H, and Supplementary Fig. E8A).

Finally, we aimed to restore FZD4 function and found that FZD4 overexpression in MLE12 cells induced *Eln* transcript and was able to rescue the CSE-induced elastin reduction (Fig. 6I), however, *Igf1* expression was below detection limit in this cell line. As such, we used pmATII cells and utilized valproic acid (VA), which has been reported to induce FZD4 expression (29). Treatment of pmATII cells with VA led to a significant increase in *Fzd4* (but not *Fzd5* or *8*) transcript (Supplementary Fig. E9A), along with *Axin2* induction (Supplementary Fig. E9A). As expected, induction of Wnt/ $\beta$ -catenin signaling by VA was diminished by co-treatment with the FZD4 inhibitor as measured with TOP/FOP flash activity (Supplementary Fig. E9B). Accordingly, we found an increase in *Fzd4* and *Axin2* by VA treatment in *ex vivo* mouse 3D-LTCs (Fig. 6J) and while *Igf1* transcript was not significantly induced at this time point, we detected a significant increase in IGF1 protein upon VA treatment *ex vivo* (Fig. 6K). Taken together, these data support the notion that FZD4 signaling is involved in elastic matrix composition.

## Discussion

Here, we report reduced expression of the FZD4 receptor in COPD patients as well as two independent animal models of COPD. We demonstrate for the first time to our knowledge that downregulation of FZD4 within the alveolar epithelium is mediated by cigarette smoke *in vitro* and *in vivo*, leading to loss of WNT/ $\beta$ -catenin signal activity and subsequently reduced lung tissue repair. We show that FZD4 reduction diminishes alveolar epithelial cell wound repair capacity and contributes to reduced elastogenic component expression, features of COPD pathogenesis, and thus might represent a potential therapeutic target (Fig. 7).

Loss of functional parenchymal lung tissue is a main feature of COPD, however, the underlying mechanisms are still poorly understood. Altered WNT signal activity has been linked to COPD (13-16, 30, 31). It has been shown that WNT/ $\beta$ -catenin signaling is reduced in the lung epithelium in COPD and that this contributes to diminished tissue repair (13, 14) as well as airway inflammation (32). Notably, we have recently demonstrated that activation of WNT/ $\beta$ -catenin is feasible in patient-derived human lung tissue cultures (3D-LTCs) and induces alveolar epithelial cell activation (14). The cause for WNT/ $\beta$ -catenin signal reduction in emphysema and a potential involvement of specific WNT/ $\beta$ -catenin receptors, however, remains elusive.

WNT signaling is regulated by a large number of different, but structurally similar, WNT ligands and FZD receptors. At least 19 WNT ligands and 10 membrane-bound FZD receptors are described to transduce intracellular WNT signaling via a number of co-receptors (12). WNT/FZD interactions are proposed to be highly context dependent, however, our knowledge of specific WNT/FZD pairs remains limited (33). To date, there are

no studies investigating the functional influence of FZD4 on WNT signaling neither in the lung, nor in general. FZD4 has been reported to be involved in angiogenesis in the eye with FZD4 mutation in humans being responsible for incomplete retinal vascularization in familial exudative vitreoretinopathy (34, 35). Here, we initially found FZD4 expression to be enriched in the alveolar epithelium and show that FZD4 expression is altered by CS *in vitro* and *in vivo*. Similarly, Guo *et al.* have recently reported reduced *FZD4* mRNA in a CS-exposed bronchial epithelial cell line *in vitro* (30). Notably, expression analysis in our cohort of never-smokers, smokers and COPD patients, revealed that FZD4 expression is even further decreased in late stage COPD patients compared to smokers, suggesting additional COPD-related mechanisms driving FZD4 reduction.

COPD has been proposed to be a disease of accelerated aging (36). Interestingly, *FZD4* expression correlated with age in the human and murine lung, further indicating that WNT signaling also impacts aging processes and might be involved in cellular senescence (36, 37). We have recently reported a canonical to non-canonical WNT signal switch in COPD (38), which might be driven by aging (39). We provide several lines of evidence that FZD4 is mainly mediating canonical WNT/ $\beta$ -catenin signaling, which is in line with previous reports (33, 40), and thus suggesting that FZD4 reduction might contribute to a WNT signal shift by inhibiting WNT/ $\beta$ -catenin signaling. Nevertheless, we cannot rule out that FZD4 reduction also impacts non-canonical WNT signaling and further studies are needed to shed light onto WNT receptor mediating non-canonical WNT signaling in alveolar epithelial cell repair.

ATII cells play a major role in lung homeostasis and can furthermore serve as a progenitor pool for ATII and ATI cells after alveolar injury (41, 42). Gain-and loss of function studies of FZD4 not only modulated WNT/ $\beta$ -catenin signaling in alveolar epithelial cells, but further led to several functional effects, such as wound healing, differentiation of the



alveolar epithelium as well as organoid formation. These data are in line with previous findings describing an imbalance of alveolar epithelial cell apoptosis/proliferation in end-stage emphysema (43) and strongly indicate that FZD4 signaling is relevant for alveolar epithelial cell repair.

Breakdown of elastic fibers in the lung is one of the main features of COPD and overall alveolar fiber content has been shown to positively correlate with lung function parameters (44). Elastic fibers are insoluble extracellular matrix (ECM) assemblies that consist of an elastin core and a mantle of fibrillin-rich microfibrils (45). Cross-linking of tropoelastin monomers, a critical step to generate an insoluble elastin polymer, is initiated by the lysyl oxidase family of enzymes (Lox and Loxl 1-4). Inflammatory mediators such as macrophage elastase (MMP-12) can modulate elastin gene expression and subsequently decrease accumulation of elastic fibers in tissues (6, 7). CS is known to increase the elastolytic activity of macrophages (25, 46), impair the production of lysyl oxidase and alter elastin re-synthesis in elastase-induced emphysema (47) and has been shown to decrease protein elastin content *in vivo* (48). Similarly, we observed that CS decreased elastin expression in a COPD model *in vivo* and downregulated expression of elastogenic components, such as Loxl, *in vitro*. Notably, blocking of FZD4 mimicked this alteration in alveolar epithelial cells *in vitro*. Moreover, IGF1, which is an epithelial cell-derived proelastogenic cytokine reduced in COPD (49-51), was also reduced upon both CSE and FZD4 blockade. To evaluate the potential role for FZD4 signaling to enhance lung repair processes, we applied two different approaches, FZD overexpression *in vitro* and induction of FZD4 by valproic acid (VA) *ex vivo*. FZD4 overexpression was able to rescue the CSE-induced decrease in elastin expression, however we could not detect all elastogenic components in the used cell line. VA is an FDA approved drug for seizures, and manic or

mixed episodes associated with bipolar disorder. It has been linked to increases in FZD4 expression (29) and could be used for treatment of primary cells and tissue. VA treatment led to FZD4-dependent induction of WNT signal activity and increased expression of IGF1, decreased in COPD patients (49-51). However, we cannot exclude that VA additionally acts on other signaling pathways contributing to the observed effects.

FZD4 is the first WNT receptor that we identified to be involved in alveolar epithelial cell repair. Recently, it has been reported that FZD8 is expressed by lung fibroblast and exhibits a pro-inflammatory role in chronic bronchitis (31). Moreover, we found that FZD8 on fibroblasts also mediates pro-fibrotic TGF- $\beta$  signaling in lung fibrosis (52). Our data suggest that other FZD receptor are also differentially regulated in COPD and thus might very well be involved in mechanisms of lung injury and repair. One can hypothesize that these FZDs might be enriched and/or regulated on other cell types, such as mesenchymal or inflammatory cells, that are further needed for proper lung repair. Distinct WNT/FZD signals seem to be cell-specific, thus highlighting the potential of these membrane-bound receptors as therapeutic targets.

The study presented here identifies reduced FZD4 signaling as an important contributor to impaired lung repair in COPD using several different experimental setups *in vivo*, *ex vivo* and *in vitro*. Certain limitations of the study, however, require further investigations. COPD is a very complex disease with several factors contributing to the pathogenesis. In this study, we mainly focus on the impact of the main risk factor cigarette smoke on FZD4 expression and subsequent alveolar epithelial cell repair, however, the role of FZD4 needs to be explored further in the context of other hallmarks of COPD, such as inflammation and tissue remodeling. We confirmed that FZD4 impacts WNT/ $\beta$ -catenin signaling and elastogenic mediators in 3D *ex vivo* lung tissue cultures (3D-LTCs) from

precision lung cut slices (PCLS), which enables the investigation within the intact 3D lung architecture and presence of several structural cell types (14). Moreover, this novel method represents an important alternative to *in vivo* animal models. The application of 3D-LTCs holds promise to reduce overall animal experiments, thus fulfilling 3Rs (Replacement, Reduction and Refinement) recommendations from the European Parliament (53). Nevertheless, studies genetically modifying FZD4 signaling in mice *in vivo* will be of high interest to further elucidate feature of lung tissue repair including changes in elastic fiber composition and corroborate the FZD4 as a potential therapeutic target for COPD.

**Acknowledgments**

The authors are grateful to all members of the Königshoff Laboratory for stimulating discussions, to Anastasia van den Berg, Julia Kipp, Nadine Adam, Rabea Imker and Maria Magdalena Stein for excellent technical assistance and primary ATII cells isolation. We thank Christina Lucas and Korbinian Berschneider for providing CSE. We are thankful to Yukiko Tando and Mitsuhiro Yamada from Tohoku University Graduate School of Medicine, Sendai, Japan for their input. Fzd4-GFP was a gift from Robert Lefkowitz & Jeremy Nathans (Addgene plasmid #42197).

## References

1. Sullivan SD, Ramsey SD, Lee TA. The economic burden of COPD. *Chest* 2000; 117: 5S-9S.
2. Hogg JC. Pathophysiology of airflow limitation in chronic obstructive pulmonary disease. *Lancet* 2004; 364: 709-721.
3. Chung KF, Adcock IM. Multifaceted mechanisms in COPD: inflammation, immunity, and tissue repair and destruction. *Eur Respir J* 2008; 31: 1334-1356.
4. Vestbo J, Hurd SS, Agusti AG, Jones PW, Vogelmeier C, Anzueto A, Barnes PJ, Fabbri LM, Martinez FJ, Nishimura M, Stockley RA, Sin DD, Rodriguez-Roisin R. Global strategy for the diagnosis, management, and prevention of chronic obstructive pulmonary disease: GOLD executive summary. *Am J Respir Crit Care Med* 2013; 187: 347-365.
5. Seys LJ, Verhamme FM, Schinwald A, Hammad H, Cunoosamy DM, Bantsimba-Malanda C, Sabirsh A, McCall E, Flavell L, Herbst R, Provoost S, Lambrecht BN, Joos GF, Brusselle GG, Bracke KR. Role of B Cell-Activating Factor in Chronic Obstructive Pulmonary Disease. *Am J Respir Crit Care Med* 2015; 192: 706-718.
6. Taraseviciene-Stewart L, Voelkel NF. Molecular pathogenesis of emphysema. *J Clin Invest* 2008; 118: 394-402.
7. Tudor RM, Petrache I. Pathogenesis of chronic obstructive pulmonary disease. *J Clin Invest* 2012; 122: 2749-2755.
8. Sharafkhaneh A, Hanania NA, Kim V. Pathogenesis of emphysema: from the bench to the bedside. *Proc Am Thorac Soc* 2008; 5: 475-477.
9. Boucherat O, Morissette MC, Provencher S, Bonnet S, Maltais F. Bridging Lung Development with Chronic Obstructive Pulmonary Disease. Relevance of Developmental Pathways in Chronic Obstructive Pulmonary Disease Pathogenesis. *Am J Respir Crit Care Med* 2016; 193: 362-375.
10. Konigshoff M, Eickelberg O. WNT signaling in lung disease: a failure or a regeneration signal? *Am J Respir Cell Mol Biol* 2010; 42: 21-31.
11. Cardoso WV, Lu J. Regulation of early lung morphogenesis: questions, facts and controversies. *Development* 2006; 133: 1611-1624.
12. Logan CY, Nusse R. The Wnt signaling pathway in development and disease. *Annu Rev Cell Dev Biol* 2004; 20: 781-810.
13. Kneidinger N, Yildirim AO, Callegari J, Takenaka S, Stein MM, Dumitrascu R, Bohla A, Bracke KR, Morty RE, Brusselle GG, Schermuly RT, Eickelberg O, Konigshoff M. Activation of the WNT/beta-catenin pathway attenuates experimental emphysema. *Am J Respir Crit Care Med* 2011; 183: 723-733.
14. Uhl FE, Vierkotten S, Wagner DE, Burgstaller G, Costa R, Koch I, Lindner M, Meiners S, Eickelberg O, Konigshoff M. Preclinical validation and imaging of Wnt-induced repair in human 3D lung tissue cultures. *Eur Respir J* 2015; 46: 1150-1166.
15. Wang R, Ahmed J, Wang G, Hassan I, Strulovici-Barel Y, Hackett NR, Crystal RG. Down-regulation of the canonical Wnt beta-catenin pathway in the airway epithelium of healthy smokers and smokers with COPD. *PLoS One* 2011; 6: e14793.
16. Jiang Z, Lao T, Qiu W, Polverino F, Gupta K, Guo F, Mancini JD, Naing ZZ, Cho MH, Castaldi PJ, Sun Y, Yu J, Lauchó-Contreras ME, Kobzik L, Raby BA, Choi AM, Perrella MA, Owen CA, Silverman EK, Zhou X. A Chronic Obstructive Pulmonary

- Disease Susceptibility Gene, FAM13A, Regulates Protein Stability of beta-catenin. *Am J Respir Crit Care Med* 2016.
17. John-Schuster G, Hager K, Conlon TM, Irmeler M, Beckers J, Eickelberg O, Yildirim AO. Cigarette smoke-induced iBALT mediates macrophage activation in a B cell-dependent manner in COPD. *Am J Physiol Lung Cell Mol Physiol* 2014; 307: L692-706.
  18. Fujino N, Ota C, Takahashi T, Suzuki T, Suzuki S, Yamada M, Nagatomi R, Kondo T, Yamaya M, Kubo H. Gene expression profiles of alveolar type II cells of chronic obstructive pulmonary disease: a case-control study. *BMJ Open* 2012; 2.
  19. Mossina A, Lukas C, Merl-Pham J, Uhl FE, Mutze K, Schamberger A, Staab-Weijnitz C, Jia J, Yildirim AO, Konigshoff M, Hauck SM, Eickelberg O, Meiners S. Cigarette smoke alters the secretome of lung epithelial cells. *Proteomics* 2016.
  20. Generoso SF, Giustiniano M, La Regina G, Bottone S, Passacantilli S, Di Maro S, Cassese H, Bruno A, Mallardo M, Dentice M, Silvestri R, Marinelli L, Sarnataro D, Bonatti S, Novellino E, Stornaiuolo M. Pharmacological folding chaperones act as allosteric ligands of Frizzled4. *Nat Chem Biol* 2015; 11: 280-286.
  21. Mutze K, Vierkotten S, Milosevic J, Eickelberg O, Konigshoff M. Enolase 1 (ENO1) and protein disulfide-isomerase associated 3 (PDIA3) regulate Wnt/beta-catenin-driven trans-differentiation of murine alveolar epithelial cells. *Dis Model Mech* 2015; 8: 877-890.
  22. Flozak AS, Lam AP, Russell S, Jain M, Peled ON, Sheppard KA, Beri R, Mutlu GM, Budinger GR, Gottardi CJ. Beta-catenin/T-cell factor signaling is activated during lung injury and promotes the survival and migration of alveolar epithelial cells. *J Biol Chem* 2010; 285: 3157-3167.
  23. Baarsma HA, Spanjer AI, Haitsma G, Engelbertink LH, Meurs H, Jonker MR, Timens W, Postma DS, Kerstjens HA, Gosens R. Activation of WNT/beta-catenin signaling in pulmonary fibroblasts by TGF-beta(1) is increased in chronic obstructive pulmonary disease. *PLoS One* 2011; 6: e25450.
  24. Starcher BC. Elastin and the lung. *Thorax* 1986; 41: 577-585.
  25. White R, White J, Janoff A. Effects of cigarette smoke on elastase secretion by murine macrophages. *J Lab Clin Med* 1979; 94: 489-499.
  26. Srisuma S, Bhattacharya S, Simon DM, Solleti SK, Tyagi S, Starcher B, Mariani TJ. Fibroblast growth factor receptors control epithelial-mesenchymal interactions necessary for alveolar elastogenesis. *Am J Respir Crit Care Med* 2010; 181: 838-850.
  27. Conn KJ, Rich CB, Jensen DE, Fontanilla MR, Bashir MM, Rosenbloom J, Foster JA. Insulin-like growth factor-I regulates transcription of the elastin gene through a putative retinoblastoma control element. A role for Sp3 acting as a repressor of elastin gene transcription. *J Biol Chem* 1996; 271: 28853-28860.
  28. Noguchi A, Nelson T. IGF-I stimulates tropoelastin synthesis in neonatal rat pulmonary fibroblasts. *Pediatr Res* 1991; 30: 248-251.
  29. Smirnova L, Block K, Sittka A, Oelgeschlager M, Seiler AE, Luch A. MicroRNA profiling as tool for in vitro developmental neurotoxicity testing: the case of sodium valproate. *PLoS One* 2014; 9: e98892.
  30. Guo L, Wang T, Wu Y, Yuan Z, Dong J, Li X, An J, Liao Z, Zhang X, Xu D, Wen FQ. WNT/beta-catenin signaling regulates cigarette smoke-induced airway inflammation via the PPARdelta/p38 pathway. *Lab Invest* 2015.
  31. Spanjer AI, Menzen MH, Dijkstra AE, van den Berge M, Boezen HM, Nickle DC, Sin DD, Bosse Y, Brandsma CA, Timens W, Postma DS, Meurs H, Heijink IH, Gosens R. A

- pro-inflammatory role for the Frizzled-8 receptor in chronic bronchitis. *Thorax* 2016.
32. Heijink IH, de Bruin HG, van den Berge M, Bennink LJ, Brandenburg SM, Gosens R, van Oosterhout AJ, Postma DS. Role of aberrant WNT signalling in the airway epithelial response to cigarette smoke in chronic obstructive pulmonary disease. *Thorax* 2013; 68: 709-716.
  33. Dijksterhuis JP, Baljinnyam B, Stanger K, Sercan HO, Ji Y, Andres O, Rubin JS, Hannoush RN, Schulte G. Systematic mapping of WNT-FZD protein interactions reveals functional selectivity by distinct WNT-FZD pairs. *J Biol Chem* 2015; 290: 6789-6798.
  34. Descamps B, Sewduth R, Ferreira Tojais N, Jaspard B, Reynaud A, Sohet F, Lacolley P, Allieres C, Lamaziere JM, Moreau C, Dufourcq P, Couffignal T, Duplaa C. Frizzled 4 regulates arterial network organization through noncanonical Wnt/planar cell polarity signaling. *Circ Res* 2012; 110: 47-58.
  35. Xu Q, Wang Y, Dabdoub A, Smallwood PM, Williams J, Woods C, Kelley MW, Jiang L, Tasman W, Zhang K, Nathans J. Vascular development in the retina and inner ear: control by Norrin and Frizzled-4, a high-affinity ligand-receptor pair. *Cell* 2004; 116: 883-895.
  36. Meiners S, Eickelberg O, Konigshoff M. Hallmarks of the ageing lung. *Eur Respir J* 2015; 45: 807-827.
  37. Lehmann M, Baarsma HA, Konigshoff M. WNT Signaling in Lung Aging and Disease. *Ann Am Thorac Soc* 2016; 13: S411-S416.
  38. Baarsma HA; Skronska-Wasek W MK, Ciolek F, Wagner DE, John-Schuster G, Heinzelmann K, Gunther A, Bracke KR, Dagouassat M, Boczkowski J, Bruselle GG, Smits R, Eickelberg O, Yildirim AO, Konigshoff K. Non-canonical WNT-5A signaling impairs endogenous lung repair in COPD. *J Exp Med* 2016 *in press*.
  39. Florian MC, Nattamai KJ, Dorr K, Marka G, Uberle B, Vas V, Eckl C, Andra I, Schiemann M, Oostendorp RA, Scharffetter-Kochanek K, Kestler HA, Zheng Y, Geiger H. A canonical to non-canonical Wnt signalling switch in haematopoietic stem-cell ageing. *Nature* 2013; 503: 392-396.
  40. Jin X, Jeon HY, Joo KM, Kim JK, Jin J, Kim SH, Kang BG, Beck S, Lee SJ, Kim JK, Park AK, Park WY, Choi YJ, Nam DH, Kim H. Frizzled 4 regulates stemness and invasiveness of migrating glioma cells established by serial intracranial transplantation. *Cancer Res* 2011; 71: 3066-3075.
  41. Rock J, Konigshoff M. Endogenous lung regeneration: potential and limitations. *Am J Respir Crit Care Med* 2012; 186: 1213-1219.
  42. Hogan BL, Barkauskas CE, Chapman HA, Epstein JA, Jain R, Hsia CC, Niklason L, Calle E, Le A, Randell SH, Rock J, Snitow M, Krummel M, Stripp BR, Vu T, White ES, Whitsett JA, Morrissey EE. Repair and regeneration of the respiratory system: complexity, plasticity, and mechanisms of lung stem cell function. *Cell Stem Cell* 2014; 15: 123-138.
  43. Calabrese F, Giacometti C, Beghe B, Rea F, Loy M, Zuin R, Marulli G, Baraldo S, Saetta M, Valente M. Marked alveolar apoptosis/proliferation imbalance in end-stage emphysema. *Respir Res* 2005; 6: 14.
  44. Cardoso WV, Sekhon HS, Hyde DM, Thurlbeck WM. Collagen and elastin in human pulmonary emphysema. *Am Rev Respir Dis* 1993; 147: 975-981.
  45. Kielty CM, Sherratt MJ, Shuttleworth CA. Elastic fibres. *J Cell Sci* 2002; 115: 2817-2828.

46. Hautamaki RD, Kobayashi DK, Senior RM, Shapiro SD. Requirement for macrophage elastase for cigarette smoke-induced emphysema in mice. *Science* 1997; 277: 2002-2004.
47. Osman M, Cantor JO, Roffman S, Keller S, Turino GM, Mandl I. Cigarette smoke impairs elastin resynthesis in lungs of hamsters with elastase-induced emphysema. *Am Rev Respir Dis* 1985; 132: 640-643.
48. Seimetz M, Parajuli N, Pichl A, Veit F, Kwapiszewska G, Weisel FC, Milger K, Egemnazarov B, Turowska A, Fuchs B, Nikam S, Roth M, Sydykov A, Medebach T, Klepetko W, Jaksch P, Dumitrascu R, Garn H, Voswinckel R, Kostin S, Seeger W, Schermuly RT, Grimminger F, Ghofrani HA, Weissmann N. Inducible NOS inhibition reverses tobacco-smoke-induced emphysema and pulmonary hypertension in mice. *Cell* 2011; 147: 293-305.
49. Papaioannou AI, Mazioti A, Kiropoulos T, Tsilioni I, Koutsokera A, Tanou K, Nikoulis DJ, Georgoulis P, Zakynthinos E, Gourgoulis KI, Kostikas K. Systemic and airway inflammation and the presence of emphysema in patients with COPD. *Respir Med* 2010; 104: 275-282.
50. Kythreotis P, Kokkini A, Avgeropoulou S, Hadjioannou A, Anastasakou E, Rasidakis A, Bakakos P. Plasma leptin and insulin-like growth factor I levels during acute exacerbations of chronic obstructive pulmonary disease. *BMC Pulm Med* 2009; 9: 11.
51. Ye M, Yu H, Yu W, Zhang G, Xiao L, Zheng X, Wu J. Evaluation of the significance of circulating insulin-like growth factor-1 and C-reactive protein in patients with chronic obstructive pulmonary disease. *J Int Med Res* 2012; 40: 1025-1035.
52. Spanjer AI, Baarsma HA, Oostenbrink LM, Jansen SR, Kuipers CC, Lindner M, Postma DS, Meurs H, Heijink IH, Gosens R, Konigshoff M. TGF-beta-induced profibrotic signaling is regulated in part by the WNT receptor Frizzled-8. *FASEB J* 2016.
53. Graham ML, Prescott MJ. The multifactorial role of the 3Rs in shifting the harm-benefit analysis in animal models of disease. *Eur J Pharmacol* 2015; 759: 19-29.



Table 1

Characteristics of study population (RT-PCR study) (n = 92)

	never smokers	smokers without COPD	COPD GOLD II	COPD GOLD III-IV
Number	18	26	34	14
Gender ratio (male/female)	6/12 #	19/7 #	31/3 #	8/6 #
Age (years)	65 (56-70)	63 (55-70)	66 (58-69)§	56 (54-60)*§†
Current- / ex-smoker	-	16/10	22/12	0/14
Smoking history (PY)	0 (0-0)	28 (15-45)*	45 (40-60)*§	30 (25-30)*†
FEV1 post (L)	2,7 (2,3-3,2)	2,7 (2,3-3,3)	2,0 (1,8-2,4)*§	0,7 (0,7-0,9)*§†
FEV1 post (% predicted)	102 (92-116)	95 (93-112)	68 (61-75)*§	26 (20-32)*§†
FEV1 / FVC post (%)	78 (75-83)	75 (71-79)*	56 (53-60)*§	32 (27-35)*§†
D <sub>LCO</sub> (% predicted)	90 (80-105)	80 (61-102)	67 (51-87)*	35 (33-41)*§†
KCO (% predicted)	103 (88-123)	91 (68-107)*	87 (62-108)*	59 (50-65)*§†
ICS (yes/no)	0/18 #	1/25 #	15/19 #	13/1 #

## Footnote

PY (pack years); FEV1 (forced expiratory volume in 1 second); FVC (forced vital capacity);  
DLCO (diffusing capacity of the lung for carbon monoxide); ICS (inhaled corticosteroids)

Data are presented as median (IQR)

Mann-Whitney U test: \*  $P < 0.05$  versus never smokers; §  $P < 0.05$  versus smokers without  
COPD; †  $P < 0.05$  versus COPD GOLD I-II

Fisher's exact test: #  $P < 0.001$

### **Figure legends**

#### **Figure 1: FZD4 is expressed in the alveolar epithelium and decreased in COPD**

(A) *Fzd* expression in whole lung homogenate obtained at day 2, 5 or 7 post PBS or Elastase instillation in C57BL/6 mice; relative gene expression  $\Delta\text{Ct}$  ( $\Delta\text{Ct} = \text{Ct Hprt} - \text{Ct gene of interest}$ ) is presented as mean  $\pm$  s.d. (n=3-6). Means were compared using one-way Anova followed by Newman-Keuls's multiple comparison test. (B) Immunofluorescence staining for FZD4 protein expression in pHATII cells. The scale bar represents 20  $\mu\text{m}$ . (C) *FZD4* gene expression in pHATII cells isolated from non-COPD and COPD patients; relative gene expression  $\Delta\text{Ct}$  is presented as mean  $\pm$  s.d. (non COPD n=7; COPD n=3). Means were compared using the Student's t-test. (D) *FZD4* expression in lung resection specimens from 92 subjects: 18 never smokers, 26 smokers without airflow limitation, 34 patients with COPD GOLD stage II and 14 patients with COPD GOLD stage III-IV; relative gene expression  $\Delta\text{Ct}$  (corrected by a normalization factor that was calculated based on the expression of the three reference genes) is presented as mean  $\pm$  s.e.m. Means were compared using Mann-Whitney U test. (E) Correlation between *FZD4* expression in the lung and the lung function parameter %FEV<sub>1</sub>. (F) Correlation between *FZD4* expression in the lung and pack-years (PY). Significance: \*p<0.05, \*\*p<0.01, \*\*\*p<0.001.

#### **Figure 2: FZD4 expression is downregulated by cigarette smoke *in vivo* and *in vitro***

(A) *Fzd4* gene expression in whole lung homogenate obtained from C57BL/6 mice exposed to filtered air (FA) or CS for 3 days or 4 months; relative gene expression  $\Delta\text{Ct}$  is presented as mean  $\pm$  s.d. (n=4-6). Means were compared using one-way Anova followed by Newman-Keuls's multiple comparison test. (B) Representative immunoblot showing FZD4 and active  $\beta$ -catenin (ABC) protein expression in whole lung homogenate obtained from C57BL/6 mice

exposed to filtered air (FA) or cigarette smoke (CS) for 3 days, quantified relatively to  $\beta$ -actin expression; data are presented as mean  $\pm$  s.d. (n=4). Means were compared using the Student's t-test. (C) Representative image of FZD4 immunofluorescence stainings on pmATII cells at day 2 of culture. The scale bar represents 20  $\mu$ m. (D) Gene expression in pmATII cells exposed to 0% or 25% cigarette smoke extract (CSE) for 24h. Gene expression  $\Delta\Delta$ Ct is presented as mean + s.d. (n=4). Means were compared using the paired Student's t-test. (E) Representative images of immunofluorescence staining for FZD4 and CDH1 (E-CAD) in pmATII cells exposed to 0% or 25% CSE for 24h; overall expression of the FZD4 protein was quantified in comparison to the number of DAPI nuclear staining, presented as mean + s.d. (n=4), 0% CSE serves as 100%. Means were compared using the paired Student's t-test. Significance: \*p<0.05, \*\*p<0.01, \*\*\*p<0.001.

### Figure 3: FZD4 is a positive regulator of canonical WNT signaling

(A) mRNA expression of canonical WNT target genes *Axin2* and *Lgr5* in pmATII cells treated with FzM1 (2.5  $\mu$ M) for 24h. Gene expression  $\Delta\Delta$ Ct is presented as mean + s.d. (n=3). Means were compared using paired Student's t-test. (B) Determination of  $\beta$ -catenin-dependent gene transcription (TOP/FOP flash assay) in MLE12 cells pre-treated with FzM1 (10  $\mu$ M) and stimulated with WNT3A (100 ng/ml); data are presented as mean + s.d. (n=3). Means were compared using one-way Anova followed by Newman-Keuls's multiple comparison test. (C) Representative immunoblot showing active  $\beta$ -catenin (ABC) protein level and LRP6 phosphorylation (pLRP6) in MLE12 cells pre-treated with FzM1 for 20 minutes and stimulated with WNT3A for 3h; quantified relatively to  $\beta$ -actin expression; data presented as mean + s.d. (n=5). Means were compared using one-way Anova followed by Newman-Keuls's multiple comparison test. (D) Determination of  $\beta$ -catenin-dependent gene

transcription in MLE12 cells transfected with empty vector (EV) or FZD4 overexpressing plasmid (OE) and treated with WNT3A (100 ng/ml); data are presented as mean + s.d. (n=3). Means were compared using one-way Anova followed by Newman-Keuls's multiple comparison test. Significance: \* $p < 0.05$ , \*\* $p < 0.01$ , \*\*\* $p < 0.001$ .

**Figure 4: FZD4 expression regulates alveolar epithelial cell proliferation and wound closure**

(A) Influence of FZD4 expression on the viability of lung epithelial cells determined by WST-1 assay in MLE12 cells treated with FzM1 (5  $\mu$ M) for 24h, data are presented as mean + s.d. (n=4). (B) MLE12 cell number after 24h treatment without or with FzM1 (5  $\mu$ M); data are presented in comparison to control (100%) as mean + s.d. (n=3). Means were compared using the Student's t-test. (C) Influence of FZD4 expression on the viability of lung epithelial cells determined by WST-1 assay in MLE12 cells transfected with EV or OE; data are presented as mean + s.d. (n=4). (D) Representative images and quantification of Ki67 immunofluorescence staining on MLE12 cells treated with DMSO (Ctrl) or FzM1; data are presented as mean + s.d. (n=3). The scale bar represents 50  $\mu$ m. (E) Representative images and quantification of Ki67 immunofluorescence staining on MLE12 cells transfected with EV or OE; data are presented as mean + s.d. (n=3). Please note the reduced baseline proliferation upon transfection in comparison to DMSO control in (D). The scale bar represents 50  $\mu$ m. (F) Representative images and quantification of wound size in MLE12 cells treated with DMSO or FzM1; data are presented as mean + s.d. (n=3). (G) Representative images and quantification of wound size in MLE12 cells transfected with EV or OE; data are presented as mean + s.d. (n=4). Significance: \* $p < 0.05$ , \*\* $p < 0.01$ , \*\*\* $p < 0.001$ .

**Figure 5: FZD4 alters ATII-to-AT1 cell trans-differentiation processes**

(A) Representative immunoblot showing protein levels of active  $\beta$ -catenin (ABC), pLRP6, T1 $\alpha$  (ATI epithelial marker) in pmATII cells treated with DMSO or FzM1 (2.5  $\mu$ M) for 24h or 72h; quantified relatively to  $\beta$ -actin expression; data are presented as mean + s.d. relatively to respective control (n=3-4). Means were compared using Student's t-test. Significance: \*p<0.05, \*\*p<0.01, \*\*\*p<0.001.

### Figure 6: FZD4 expression influences elastogenic components

(A) *Eln* gene expression in whole lung homogenate of cigarette smoke exposed mice. Relative gene expression  $\Delta$ Ct is presented as mean  $\pm$  s.d. (n=3-5). Means were compared using one-way Anova followed by Newman-Keuls's multiple comparison test. (B) *Eln* gene expression in MLE12 cells exposed to CSE or treated with FzM1. Gene expression  $\Delta\Delta$ Ct is presented as mean + s.d. (n=3-4). Means were compared using the paired Student's t-test. (C) *Eln*, *Igf1*, *Lox*, *Loxl*, *Fbln1*, *Fbln5* gene expression in pmATII cells treated with FzM1. Gene expression  $\Delta\Delta$ Ct is presented as mean + s.d. (n=3). Means were compared using the paired Student's t-test. (D) *Eln*, *Igf1*, *Lox*, *Loxl*, *Fbln1*, *Fbln5* gene expression in pmATII cells exposed to CSE. Gene expression  $\Delta\Delta$ Ct is presented as mean + s.d. (n=3). Means were compared using the paired Student's t-test. (E) Relative IGF1 protein secretion in pmATII cells exposed to CSE. Data presented as mean + s.d. (n=4). Means were compared using the paired Student's t-test. (F) Relative IGF1 protein secretion in pmATII cells treated with FzM1. Data presented as mean + s.d. (n=5). Means were compared using the paired Student's t-test. (G) *Eln* and *Igf1* gene expression in mouse PCLS exposed to CSE for 24h or 72h. Gene expression  $\Delta\Delta$ Ct is presented as mean + s.d. (n=3). Means were compared using the paired Student's t-test. (H) *Eln* and *Igf1* gene expression in mouse PCLS treated with FzM1 for 24h or 72h. Gene expression  $\Delta\Delta$ Ct is presented as mean + s.d. (n=3). Means were compared using the paired

Student's t-test. (I) *Eln* gene expression in MLE12 cells transfected with OE FZD4 and exposed to CSE; gene expression  $\Delta\Delta Ct$  is presented as mean + s.d. (n=3-5). Means were compared using one-way Anova followed by Newman-Keuls's multiple comparison test. (J) Gene expression upon VA treatment in mouse 3D-LTCs.  $\Delta\Delta Ct$  is presented as mean + s.d. (n=3). (K) Relative IGF1 protein secretion in mouse 3D-LTCs. Data presented as mean  $\pm$  s.d. (n=3). Means were compared using the paired Student's t-test. Significance: \*p<0.05, \*\*p<0.01, \*\*\*p<0.001.

**Figure 7: Schematic representation of the proposed contribution of FZD4 signaling to impaired tissue repair in COPD.**

Healthy lung: in the presence of FZD4 receptor in the alveolar lung epithelium WNT/ $\beta$ -catenin signaling maintains cell proliferation and tissue repair. COPD: decreased expression of FZD4 receptor induced by cigarette smoke and additional environmental/genetic factors, leads to reduced WNT/ $\beta$ -catenin signaling and inhibition of epithelial cell function and components of the elastic matrix, thus contributing to impaired tissue repair and emphysema development.

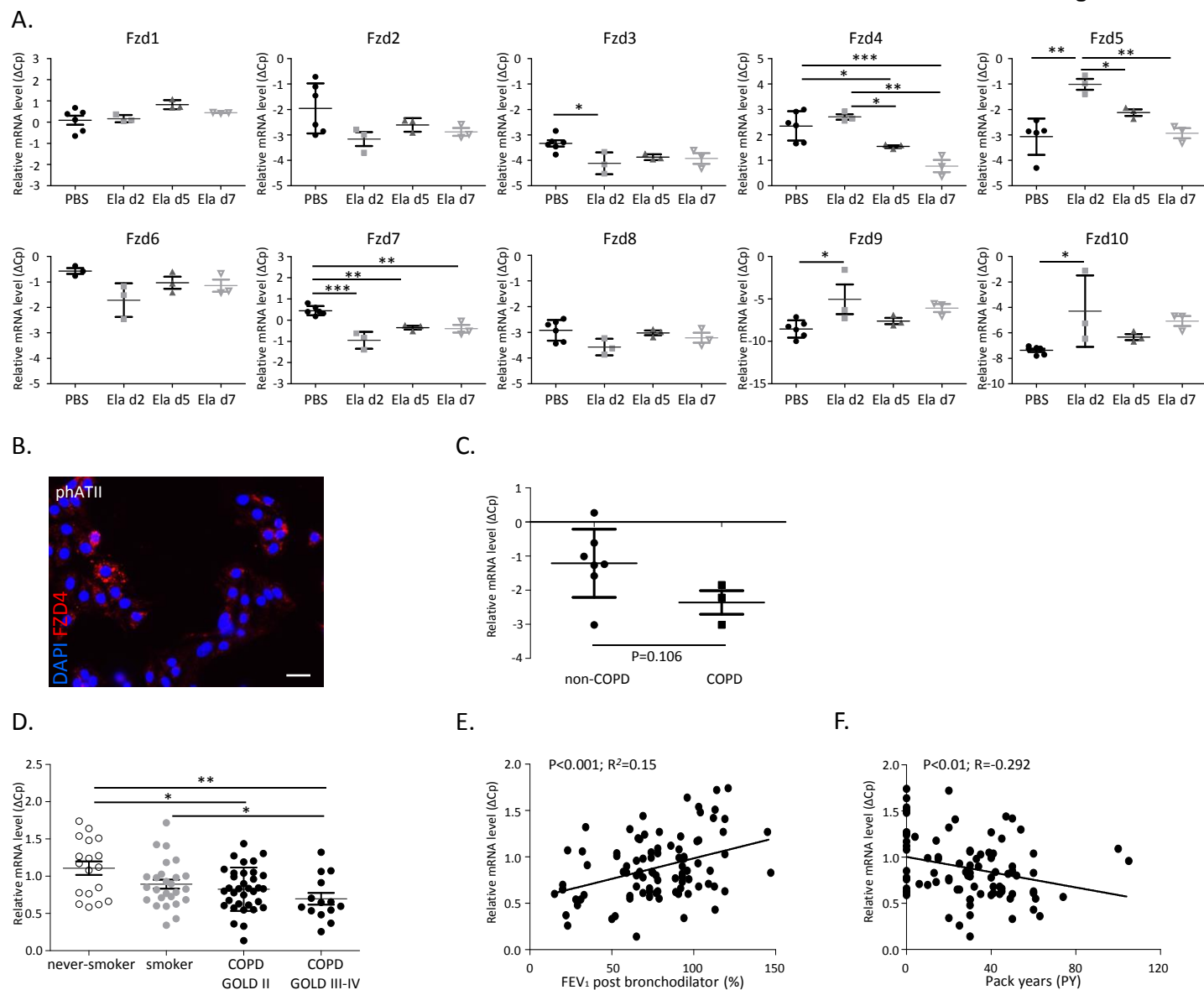
**Figure 1**




Figure 2

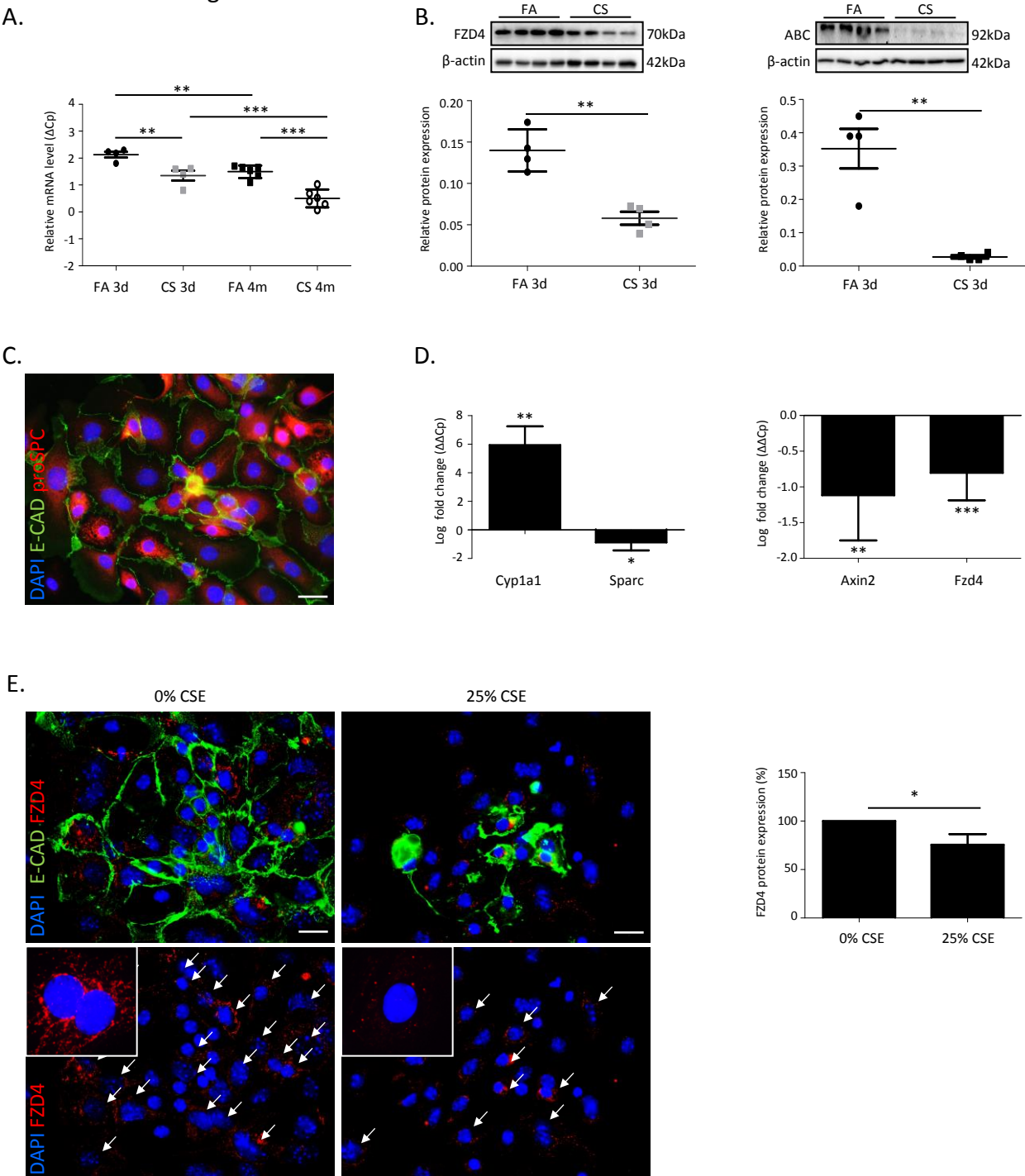
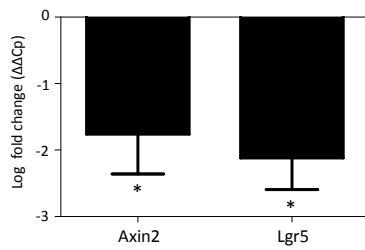
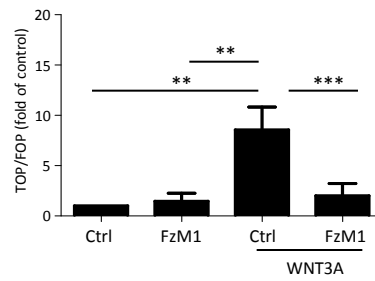


Figure 3

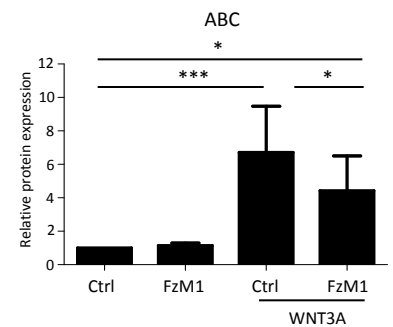
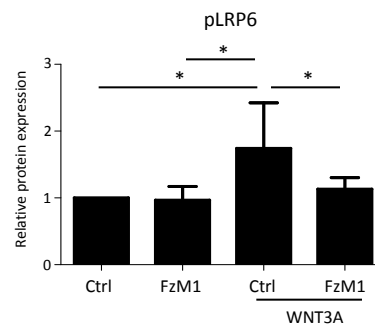
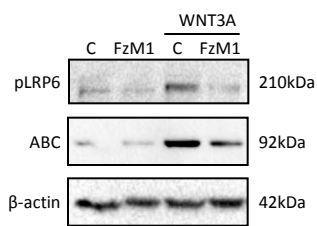
A.



B.



C.



D.

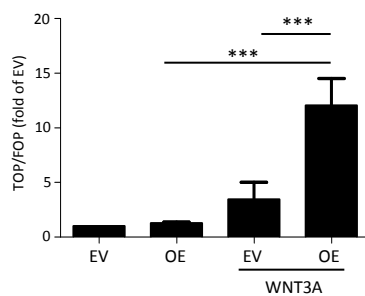


Figure 4

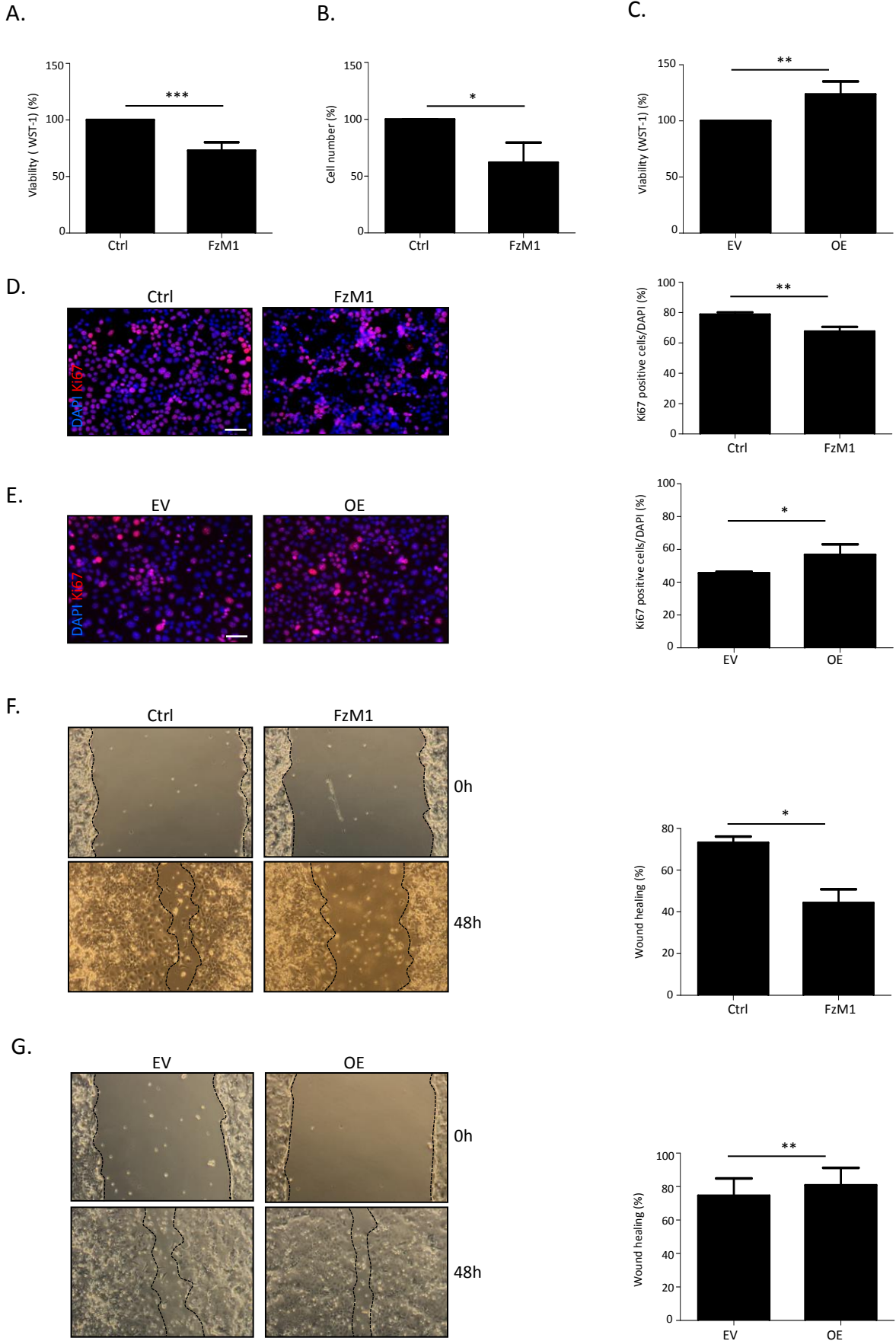


Figure 5

A.

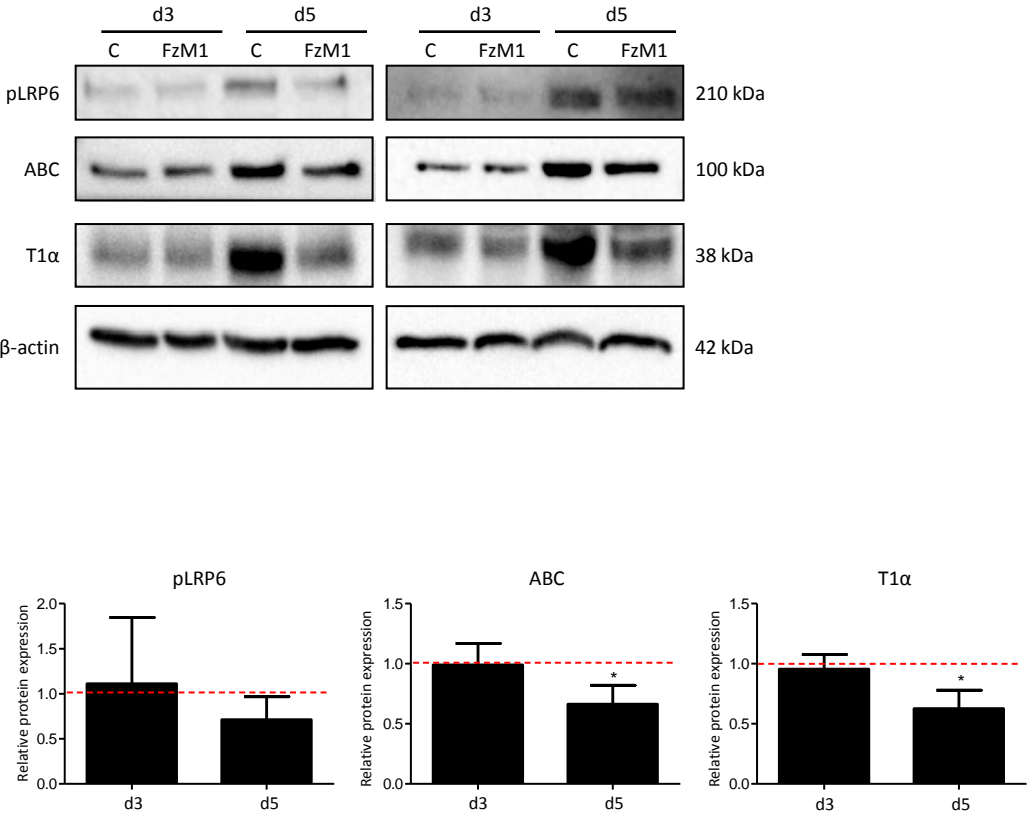
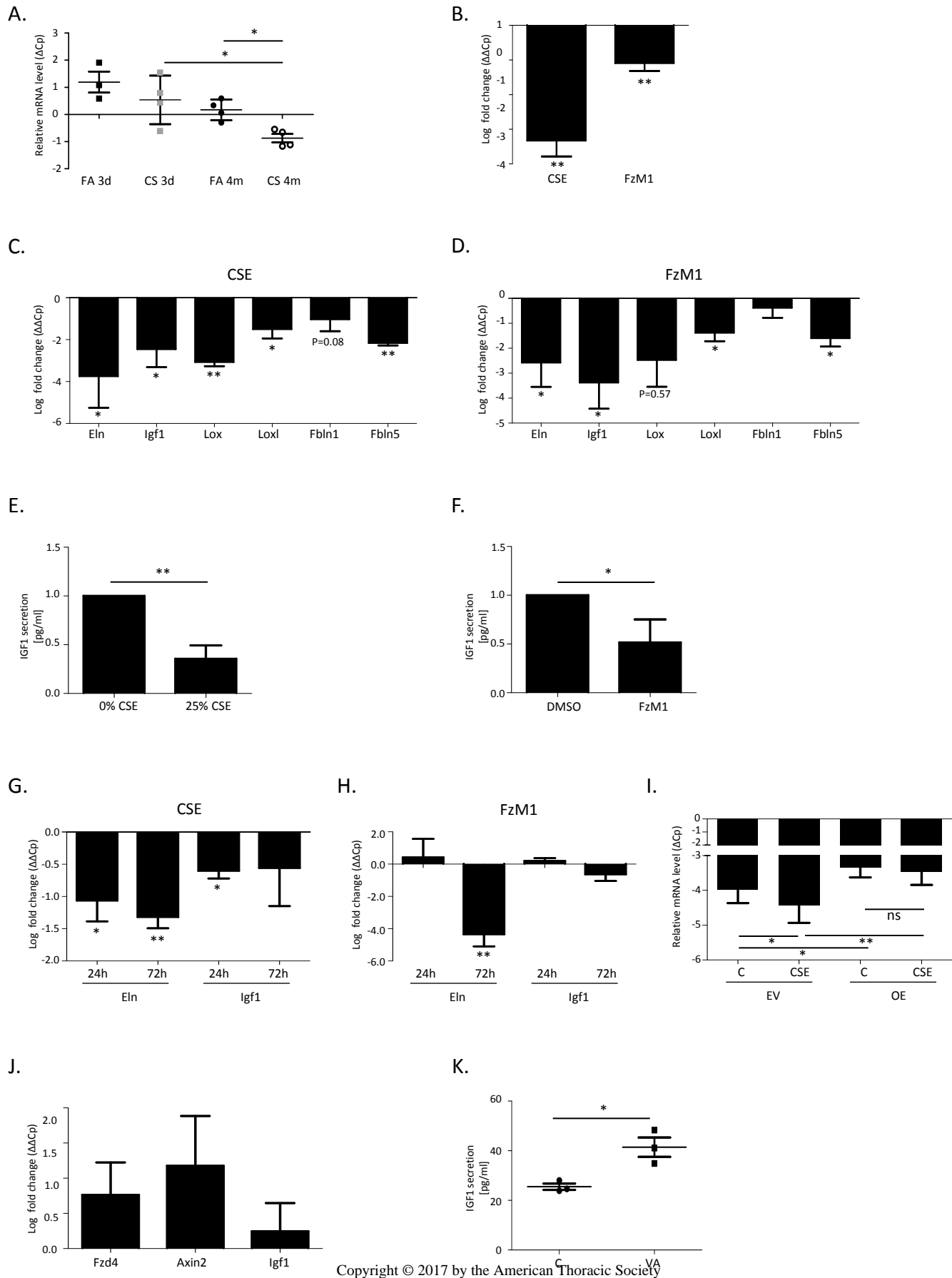
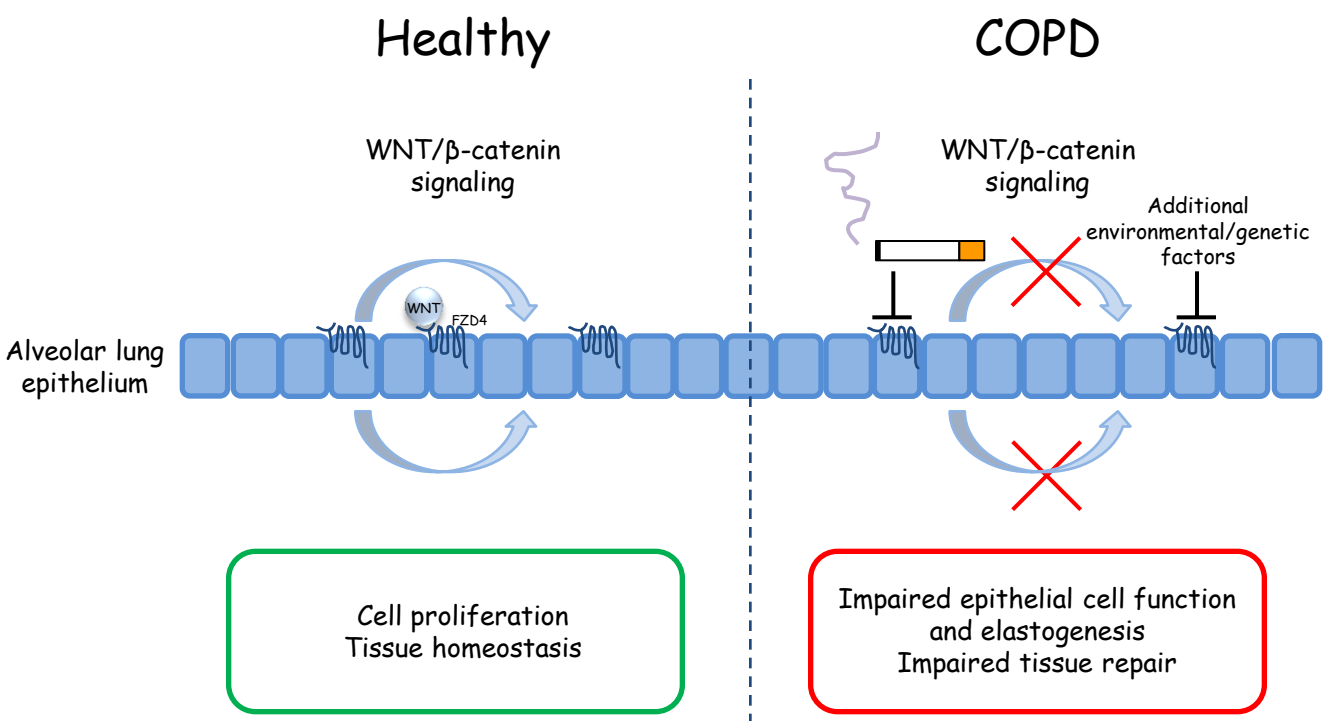


Figure 6





Online Data Supplement

Reduced Frizzled receptor 4 expression prevents WNT/ $\beta$ -catenin-driven alveolar lung repair in COPD

Wioletta Skronska-Wasek, Kathrin Mutze, Hoeke A. Baarsma, Ken R. Bracke, Hani N. Alsafadi, Mareike Lehmann, Rita Costa, Mariano Stornaiuolo, Ettore Novellino, Guy G. Brusselle, Darcy E. Wagner, Ali Ö. Yildirim, Melanie Königshoff

Table E1

Sequences of primers

Gene name	Gene sequence
<i>mAxin2</i>	5'-AGCAGAGGGACAGGAACCA-3' 5'-CACTTGCCAGTTTCTTTGGCT-3'
<i>mCdh1</i>	5'-CCATCCTCGGAATCCTTGG-3' 5'-TTTGACCACCGTTCTCCTCC-3'
<i>mCyp1a1</i>	5'-TCCTGAAGAGTGCTCTGGGT-3' 5'-TAAACCATTGTTGGGAAGGCTG-3'
<i>mElastin</i>	5'-GGCGTCTTGCTGATCCTCT-3' 5'-ATAATAGACTCCACCGGGAAC-3'
<i>mFzd1</i>	5'-AAACAGCACAGGTTCTGCAAAA-3' 5'-TGGGCCCTCTCGTTCCTT-3'
<i>mFzd2</i>	5'-TCCATCTGGTGGGTGATTCTG -3' 5'-CTCGTGGCCCCACTTCATT -3'

<i>mFzd3</i>	5'-GCCTATAGCGAGTGTTCAAACTCA -3' 5'-TGGAAACCTACTGCACTCCATATCT -3'
<i>mFzd4</i>	5'-TCCAGCCAGCTGCAGTTCTTCC -3' 5'-CTGAAAGGCACATGCCACCGC -3'
<i>mFzd5</i>	5'-CCCACCGCACGTTTTCC -3' 5'-GCTTTTCATTTGCTTCTTGTTATC -3'
<i>mFzd6</i>	5'-GTTCTACCCTGTCGGAAATTGTG -3' 5'-GTGGATGAGAAGTTACAGGAACAGTGT -3'
<i>mFzd7</i>	5'-GCCAGGTGGATGGTGACCTA -3' 5'-CCGCAATGCATCCACACTAG -3'
<i>mFzd8</i>	5'-GCAAGGAGGCCCAACTAAGAC -3' 5'-GAGGCCCAAGCGGATCA -3'
<i>mFzd9</i>	5'-CCCATCATGGAGCAATTCAATT -3' 5'-GGGAGCCGGGCACAGT -3'
<i>mFzd10</i>	5'-ACGAGATGCTGGGACTGACC-3' 5'-AACCGCATTTGGCGTTACAT-3'
<i>mHprt</i>	5'-CCTAAGATGAGCGCAAGTTGAA-3' 5'-CCACAGGACTAGAACACCTGCTAA-3'
<i>mIgf1</i>	5'-ACACCTCTTCTACCTGGCGCTC-3' 5'-ATAGCCTGTGGGCTTGTTGAAGT-3'
<i>mLgr5</i>	5'-GCGTTCACGGGCCTTCACAG-3'



	5'-GGCATCTAGGCGCAGGGATTGA-3'
<i>mLox</i>	5'-GTCACCAACATTACCACAGCATGG-3' 5'-GCCTTCAGCCACTCTCCTCTGT-3'
<i>mLoxl</i>	5'-ACTTTCTCCCCAACCGGCCA-3' 5'-CCTTGTGTCCCTCGGCTACCTT-3'
<i>mSparc</i>	5'-AAACATGGCAAGGTGTGTGA-3' 5'-AAGTGGCAGGAAGAGTCGAA-3'
<i>mT1α</i>	5'-ACAGGTGCTACTGGAGGGCTT-3' 5'-TCCTCTAAGGGAGGCTTCGTC-3'
<i>huAXIN2</i>	5'-AGAAATGCATCGCAGTGTGAAG-3' 5'-GGTGGGTTCTCGGGAAATG-3'
<i>huELN</i>	5'-GGCCATTCTGGTGGAGTTCC-3' 5'-AACTGGCTTAAGAGGTTTGCCTCC-3'
<i>huFZD4</i>	5'-GACAACTTTCACACCGCTCATC-3' 5'-CCTTCAGGACGGGTTTCA-3'
<i>huHPRT</i>	5'-AAGGACCCACGAAGTGTG-3' 5'-GGCTTTGTATTTTGCTTTTCCA-3'

Table E2

Gene Expression Assays for the housekeeping genes Applied Biosystems

Gene	ID
<i>huGAPDH</i>	Hs99999905_m1
<i>huHPRT1</i>	Hs99999909_m1
<i>huSDHA</i>	Hs00417200_m1

Table E3

Antibodies

Antibody	Company and number
Active $\beta$ -catenin (ABC)	Millipore 05-665
$\beta$ -actin	Sigma A3854
CDH1 (E-CAD)	BD 610181
Tropoelastin	Kindly provided by Dr. Robert Mecham, Washington University
FZD4	Millipore 07-2166
Ki67	Dako M7249
pLRP6	Cell signalling 2568S
T1 $\alpha$	R&D AF3244

## Online Data Supplement

### **Supplementary Figure E1: FZD4 is highly expressed in the lung epithelium and decreased in whole homogenate and phATII cells from COPD patients**

(A) *Fzd* expression in pmATII cells; relative gene expression  $\Delta\text{Ct}$  presented as mean + s.d. (n=3). (B) Immunofluorescence staining for FZD4 protein expression in pmATII cells. The scale bar represents 20  $\mu\text{m}$ . (C) *FZD* expression in whole lung homogenate of COPD patients (published microarray GSE47460); data are presented as mean  $\pm$  s.e.m. (non-COPD n=91; COPD n=144) of normalized array values. Means were compared using the Student's t-test. (D) *FZD* expression in phATII cells from non-COPD and COPD patients (published microarray GSE29133); expression of genes in COPD patients is presented relatively to non-COPD patients as mean + s.e.m. (non-COPD n=3; COPD n=3). (E) pmATII cells treated with  $\text{H}_2\text{O}_2$ , relative gene expression  $\Delta\text{Ct}$  presented as mean + s.d. (n=5). Significance: \* $p<0.05$ , \*\* $p<0.01$ , \*\*\* $p<0.001$

### **Supplementary Figure E2: Correlation between FZD4 expression and different parameters in human lung tissue (excluding COPD GOLD IV patients)**

Correlations were performed in a cohort of 92 subjects: 18 never smokers, 26 smokers without airflow limitation, 34 patients with COPD GOLD stage II and 14 patients with COPD GOLD stage III-IV; Correlation between *FZD4* mRNA expression and (A) %  $\text{FEV}_1$ , (B)  $\text{FEV}_1/\text{FVC}$ , (C) DLCO, (D) pack-years (PY), and (E) age, are depicted.

**Supplementary Figure E3: Cigarette smoke decreases canonical WNT signaling and FZD4 expression *in vivo* and *in vitro***

(A) *Fzd4* expression in the whole lung homogenates obtained from young ( $\leq 3$  months,  $n=8$ ) or old ( $\geq 12$  months,  $n=10$ ) mice. Relative gene expression  $\Delta Ct$  is presented as mean  $\pm$  s.e.m. Means were compared using the Student's t-test. (B) Immunofluorescence staining for FZD4 protein expression in human lung tissue from non smokers and smokers. The scale bar represents 20  $\mu m$ . (C) Gene expression in MLE12 cells exposed to 0% or 25% CSE for 24h. Gene expression  $\Delta\Delta Ct$  is presented as mean + s.d. ( $n=4$ ). Means were compared using the paired Student's t-test. Significance: \* $p<0.05$ , \*\* $p<0.01$ , \*\*\* $p<0.001$ . (D) Immunoblot showing FZD4 expression in pmATII cells exposed to CSE for 24h and its quantification ( $n=2$ ).

**Supplementary Figure E4: Blockade of FZD4 decreases Axin2 in human 3D-LTCs**

(A) Axin2 gene expression in human 3D-LTCs upon FZD4 blockade with FzM1, presented as  $\Delta Ct$  ( $n=3$ ) and the effect assessed with Student's t-test. Significance: \* $p<0.05$ , \*\* $p<0.01$ , \*\*\* $p<0.001$ .

**Supplementary Figure E5: FZD4 overexpression efficiency**

FZD4 overexpression efficiency was evaluated by (A) qPCR, gene expression is presented as  $\Delta Ct$  and (B) immunofluorescence staining on MLE12 cells. Means were compared using one-way Anova followed by Newman-Keuls's multiple comparison test. Significance: \* $p<0.05$ , \*\* $p<0.01$ , \*\*\* $p<0.001$ .

**Supplementary Figure E6: FZD4 inhibition by FzM1 negatively regulates the expression of epithelial markers in pmATII cells and inhibits organoid formation**

(A) *E-cadherin (Cdh1)* and *T1a* epithelial marker expression was measured in pmATII cells stimulated with FzM1 (n=3) by qPCR. Gene expression is presented as mean + s.d. Means were compared using the paired Student's t-test. (B) Representative pictures of organoids formed by pmATII cells at day 7 of culture and quantification of organoid numbers. Data presented as mean + s.d. (n=3). Means were compared using the paired Student's t-test. Significance: \*p<0.05, \*\*p<0.01, \*\*\*p<0.001.

**Supplementary Figure E7: Elastin expression in the lung**

(A) Immunoblot showing Tropoelastin protein expression in cultured pmATII cells at day 4 and in mouse lung homogenate.

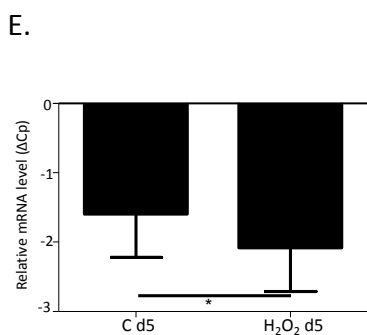
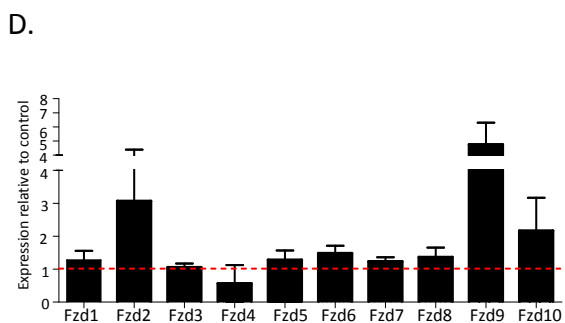
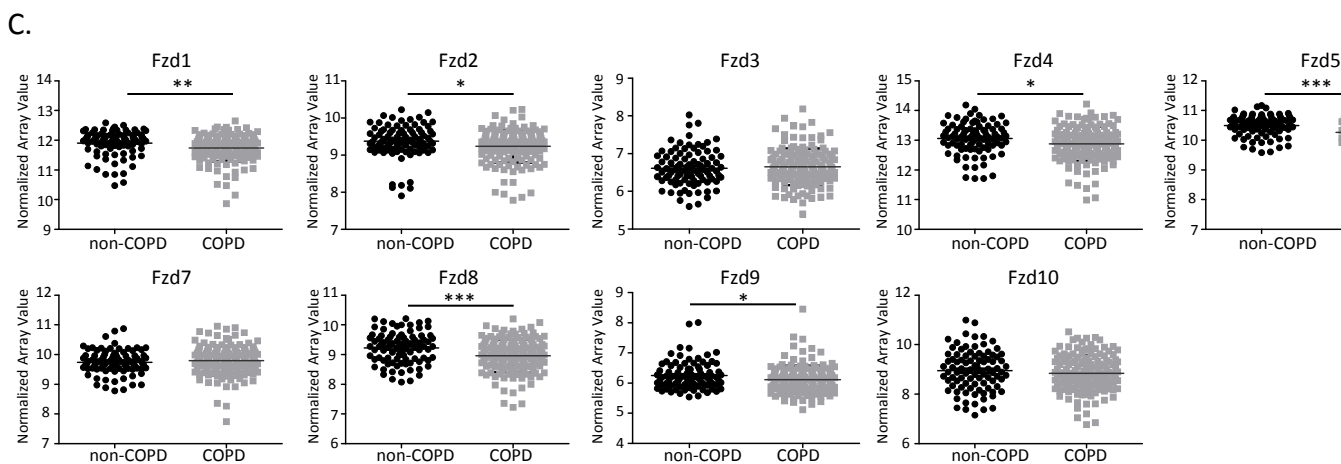
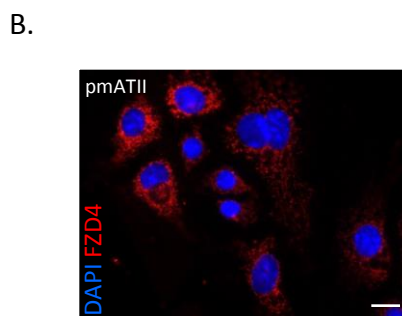
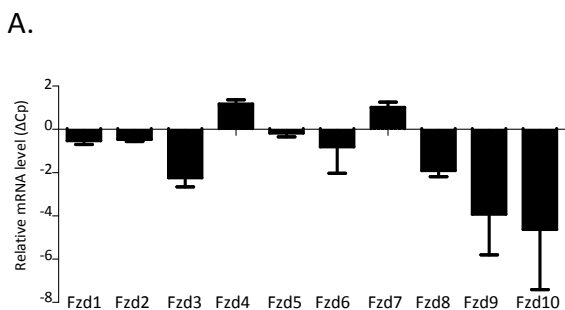
**Supplementary Figure E8: Cigarette smoke effect on 3D-LTCs**

(A) *Cyp1a1* and *Sparc* gene expression in mouse 3D-LTCs generated from precision cut lung slices exposed to CSE for 24h or 72h. Gene expression  $\Delta\Delta Ct$  presented as mean + s.d. (n=3). Means were compared using the paired Student's t-test. Significance: \*p<0.05, \*\*p<0.01, \*\*\*p<0.001.

**Supplementary Figure E9: VA induces FZD4 expression and WNT signaling in lung epithelial cells**

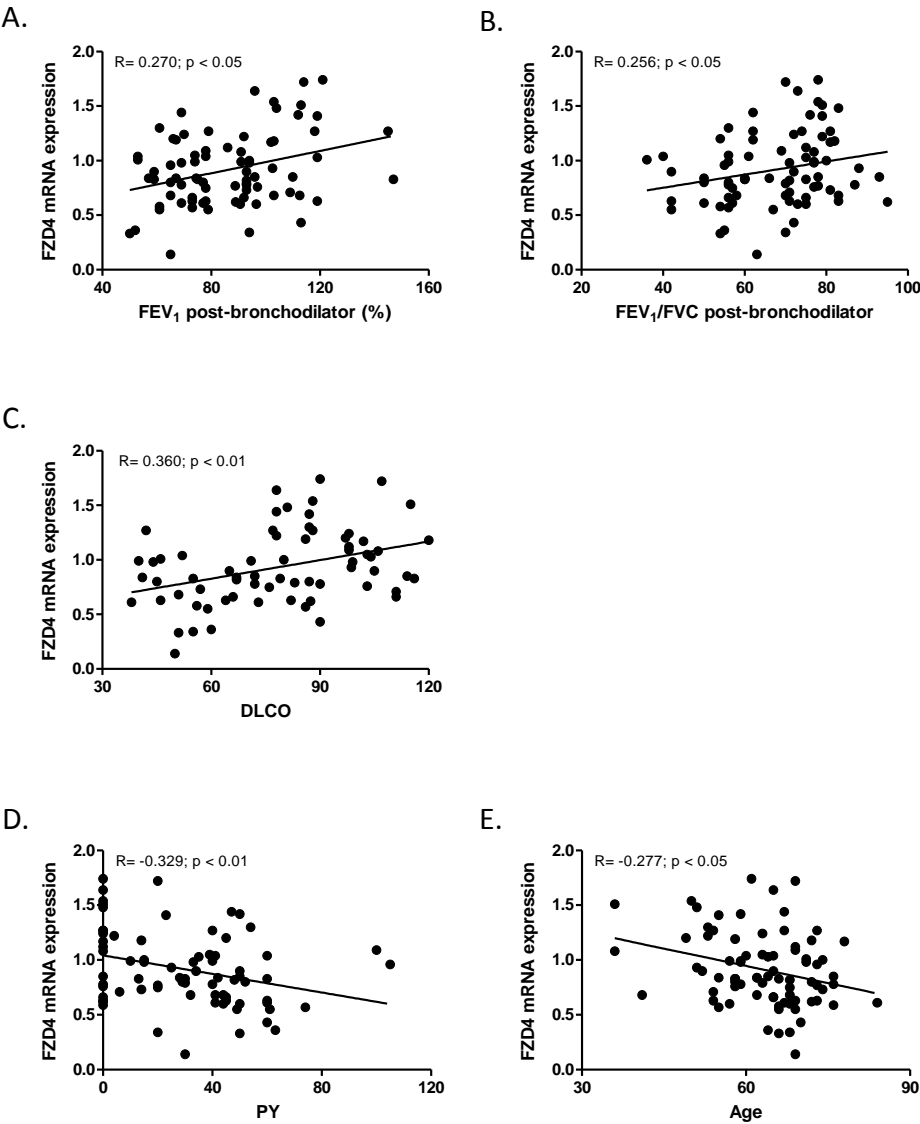
(A) *Fzd 4, 5, 8* and *Axin2* gene expression in pmATII cells treated with VA for 24h. Relative gene expression  $\Delta Ct$  presented as mean + s.d. (n=3). (B) Determination of  $\beta$ -catenin-dependent gene transcription (TOP/FOP flash assay) in MLE12 cells

stimulated with FzM1, VA or combination thereof for 24h. Data presented as mean + s.d. (n=3). Means were compared using one-way Anova followed by Newman-Keuls's multiple comparison test. Significance: \* $p < 0.05$ , \*\* $p < 0.01$ , \*\*\* $p < 0.001$ .

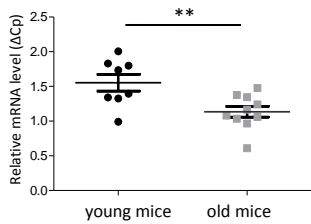




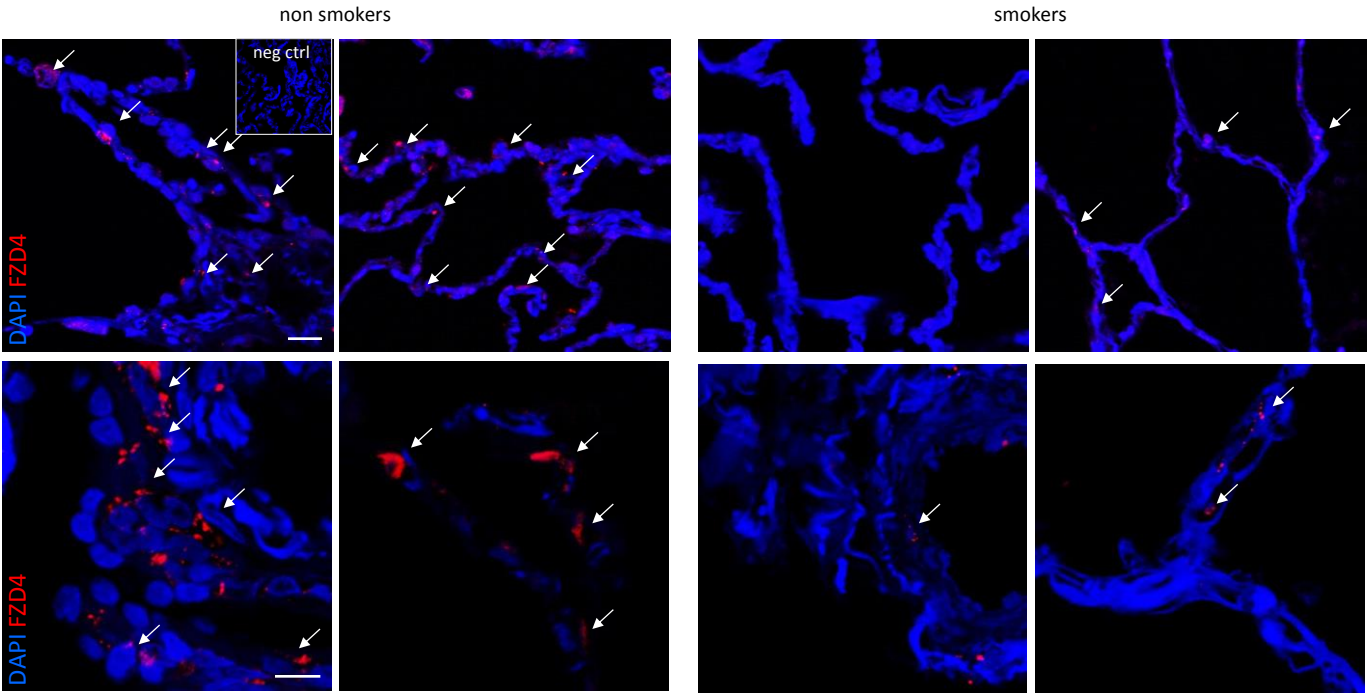
Supplementary Figure E2



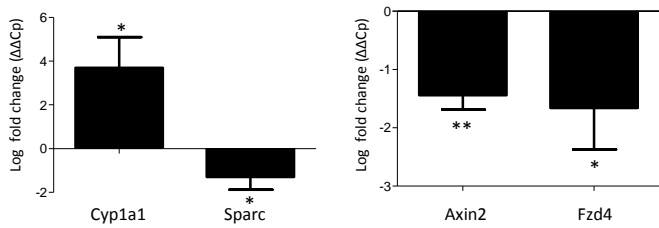
A.



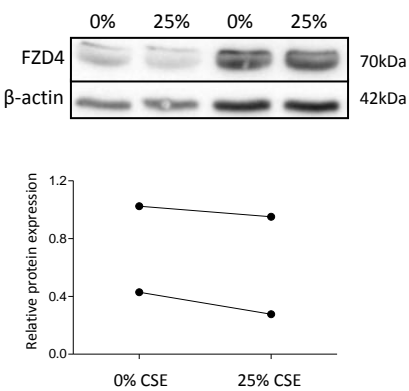
B.



C.

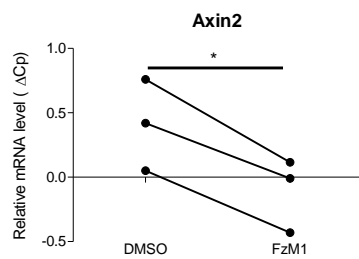


D.



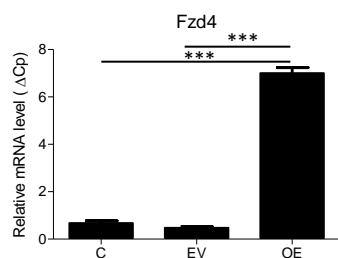
## Supplementary Figure E4

A.

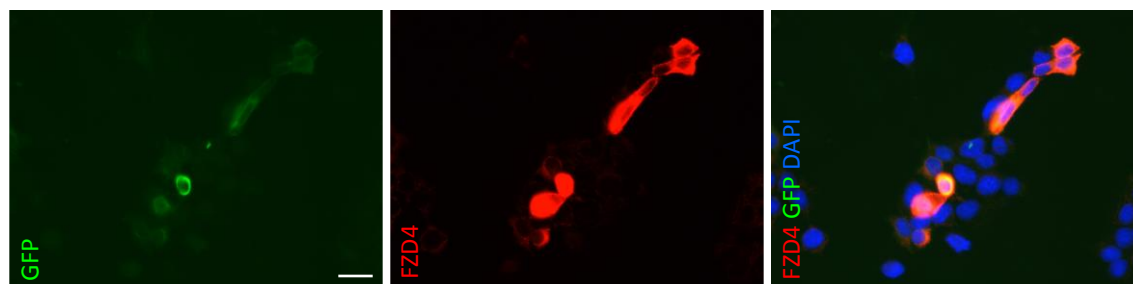


# Supplementary Figure E5

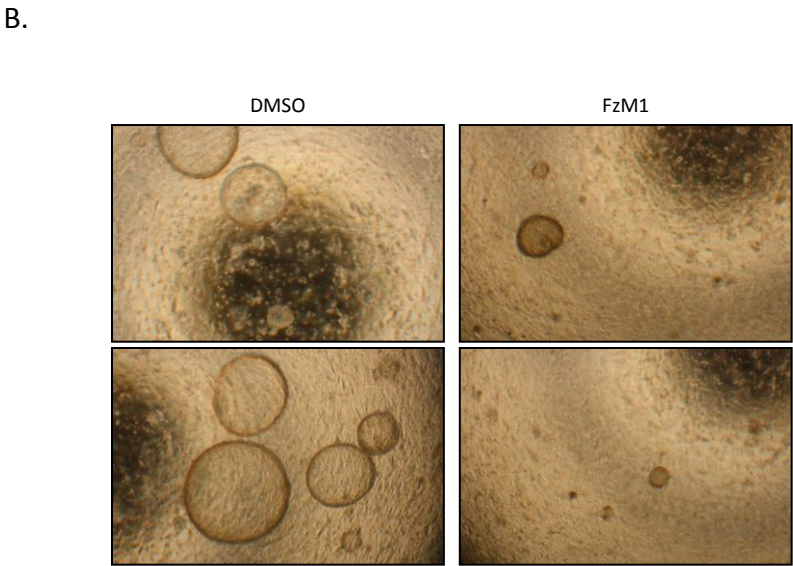
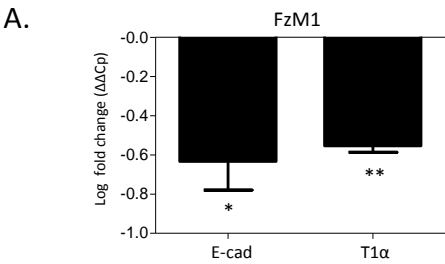
A.



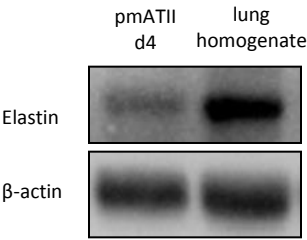
B.



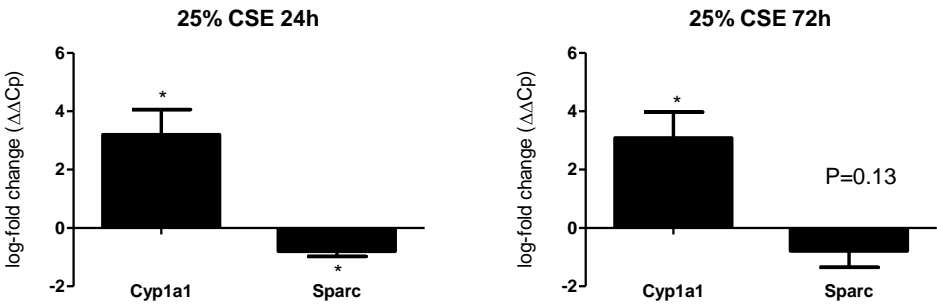
Supplementary Figure E6



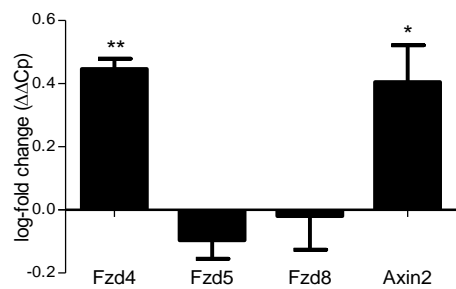
A.



A.                      Supplementary Figure E8



A.



B.

